

Dangerous Angular KK/Glueball Relics in String Theory Cosmology

J.F. Dufaux^{1,2}, L. Kofman², M. Peloso³

¹ *Instituto de Física Teórica UAM/CSIC,*

Universidad Autónoma de Madrid, Cantoblanco, 28049 Madrid, Spain

² *CITA, University of Toronto, 60 St. George st.,*

Toronto, ON M5S 3H8, Canada and

³ *School of Physics and Astronomy,*

University of Minnesota, Minneapolis, MN 55455, USA

(Dated: February 18, 2022)

Abstract

The presence of Kaluza-Klein particles in the universe is a potential manifestation of string theory cosmology. In general, they can be present in the high temperature bath of the early universe. In particular examples, string theory inflation often ends with brane-antibrane annihilation followed by the energy cascading through massive closed string loops to KK modes which then decay into lighter standard model particles. However, massive KK modes in the early universe may become dangerous cosmological relics if the inner manifold contains warped throat(s) with approximate isometries. In the complimentary picture, in the AdS/CFT dual gauge theory with extra isometries, massive glueballs of various spins become the dangerous cosmological relics. The decay of these angular KK modes/glueballs, located around the tip of the throat, is caused by isometry breaking which results from gluing the throat to the compact CY manifold. We address the problem of these angular KK particles/glueballs, studying their interactions and decay channels, from the theory side, and the resulting cosmological constraints on the warped compactification parameters, from the phenomenology side. The abundance and decay time of the long-lived non-relativistic angular KK modes depend strongly on the parameters of the warped geometry, so that observational constraints rule out a significant fraction of the parameter space.

I. INTRODUCTION

Often when we embed a new layer of elementary particle theory in the theory of the early universe, we find that new particles become dangerous cosmological relics. The study of this problem is one of the few tools available for theorists to bridge these two theories. For example, the GUT theory incorporated in the Hot Big Bang model predicted the overproduction of monopoles; SUGRA theory predicted the overproduction of gravitinos and moduli fields. It is interesting to explore if the embedding of string theory in cosmology results in new dangerous relics.

Kaluza-Klein (KK) particles in the universe is a possible signature of string theory physics. Relic KK particles may be good or bad for cosmology, depending on their properties. If their abundance multiplied by their mass is tuned to be right, and their life time is significantly longer than the age of the universe, the KK particles can be dark matter candidates. Otherwise, and more typically, they are dangerous relics, which may overclose the universe, or violate Big Bang Nucleosynthesis or other astrophysical constraints, depending on their abundance and lifetime. Therefore, the theory of relic KK particles is a powerful tool to study string theory cosmology and to confront it with observations.

The AdS/CFT duality allows us to translate from the language of the gravitational KK sector to gauge theories. Therefore, independently of string theory, the story of dangerous cosmological relics repeats itself in the context of gauge theories with extra isometries, which contain massive glueballs of different spins.

We will consider KK particles in a string theory and string theory cosmology setting, which drew significant interest in the last few years, and which can be advanced quantitatively. Indeed, important progress has been made in the studying type IIB string theory compactifications with fluxes where the moduli are stabilized [1, 2]. These developments in string theory have raised interests in the embedding of early universe inflation and low energy physics in a fundamental and phenomenologically viable framework.

Constructions with fluxes and conifolds induce warped regions of spacetime [1, 3, 4] - throats - which in turn may be used to generate mass hierarchies. For instance, the hierarchy between the string scale and the electroweak scale may be generated à la Randall-Sundrum [5] when the Standard Model degrees of freedom are localized at the bottom of a sufficiently warped throat. Furthermore, warping is an essential ingredient in the attempts

to realize brane inflation in the slow-roll regime [6] or the DBI regime [7], or in the fast-roll regime [8], see also e.g. [9, 10, 11] for recent works.

Warped brane/anti-brane inflation involves a pair of brane/anti-brane $D3$ and $\bar{D}3$, which are string theory objects: although inflation in this model may be described with an effective four dimensional field theory, its end point, reheating, is associated with the $D3-\bar{D}3$ annihilation, which is not captured by field theory. Reheating from brane/anti-brane annihilation is rather different from (p)reheating in quantum field theory [12], and was investigated in several papers [13, 14, 15, 16, 17], which identified the channels of inflaton energy decay, cascading from tachyon annihilation to the lighter standard model particles through massive closed string loops, KK modes, and brane displacement moduli. Indeed, if the internal space has warped regions (throats), the mass of the KK modes associated with them is much lower than the fundamental scale, being redshifted by the warp factor at the bottom of the throat. If the KK modes are sufficiently light then it is natural to expect them to be produced during reheating. For instance, in models of brane/anti-brane inflation, KK modes are copiously produced by the decay of the closed string loops from the brane/anti-brane annihilation at the end of inflation, and their energy must be efficiently converted into Standard Model (SM) degrees of freedom.

Notably, reheating is then bottlenecked through KK modes which are localized around the tip of the throat. Warped brane inflation and reheating after brane annihilation were considered for throat models with high isometries, often described by the Klebanov-Strassler (KS) solution [3]. The KS geometry has $S0(4) \times \mathbb{Z}_2$ isometries around the tip of the throat, and it is close to $AdS_5 \times T^{1,1}$ away from the tip. Other known examples of throat solutions also have similar isometries [18]. To make the inner space compact, the KS throat is glued to the unwarped Calabi-Yau (CY) part of the manifold. For cosmologists, a significant advantage of this model is that the metric of the throat is known analytically, so that KK modes can be studied in some detail. However, as it was found in [14], the advantage in mathematics is in this case a disadvantage in physics. Indeed, the KK modes in internal spaces with isometries have conserved angular momentum quantum numbers associated with these isometries. The final decay products of the KK particles, the SM particles, do not have such quantum numbers. Therefore KK modes with (internal) angular momenta cannot decay into SM particles. Moreover, KK particles with opposite angular momenta cannot annihilate completely into SM particles due to the expansion of the universe. Therefore, we

encounter the severe problem that the frozen out fraction of the long-lived angular Kaluza-Klein modes can overclose the universe [14]¹! The problem of angular KK modes from an inner geometry with throats is not specific to the warped brane/anti-brane inflationary scenario. Independently on the particular realization of inflation, light KK modes may be produced during reheating if they are sufficiently coupled to inflation. In any context where the reheat temperature of the very early universe is large enough, massive KK particles can be produced in the thermal bath. Then, KK modes with angular momenta will again freeze out, and can be dangerous for cosmology.

In a sense, the problem of dangerous angular KK modes in string theory cosmology is a re-appearance of the problem of KK modes from dimensional reduction in supergravity in higher dimensions with isometries [20]. However, the string theory setting brings new features in cosmology with KK modes. The unwarped CY part of the compact manifold does not preserve the isometries of the throat. Therefore, when we embed the KS throat into the compact manifold, the isometries of the throat inevitably get broken. These deviations from isometries are significant at the base of the throat, close to the unwarped CY, but they decrease exponentially towards the tip of the throat. On the other hand, the KK modes are localized at the tip of the throat and their wave functions decrease exponentially towards the base. The net effect will be some violation of the conservation of the angular momentum of the KK modes. In terms of the four-dimensional effective lagrangian, this manifests itself by additional terms describing the decay of angular KK modes into SM particles with small coupling constants, controlled by the isometry breaking. This makes angular KK modes in the universe not stable but short or long lived, depending on the parameters of the model.

In this paper, we investigate in some detail the decay of Kaluza-Klein modes with angular momenta associated with the compact manifold in warped flux compactifications, namely, in a KS throat with broken isometries. In Section II we begin with the background throat geometry; we consider first the KS solution with intact isometries, and we then introduce the isometry breaking. We use the static perturbations of the KS metric considered in [21], where they were connected to symmetry breaking operators in the context of the AdS/CFT

¹ It turns out that the left-over abundance of angular KK modes is very sensitive to the parameters of the throat geometry. Alternatively, after tuning the parameters, these modes have been proposed as possible dark matter candidates [14], [15] (see also [19] for earlier proposals of KK dark matter, in the context of other models).

correspondence.

In Section III we consider the wave functions of the KK modes in the throat geometry. For definiteness we will discuss the gravi-tensor KK modes (the spin-two KK modes, or spin-two glueballs). The knowledge of the wave functions allows us to integrate the internal space out, and to study the effective four-dimensional physics of the model. From the spectroscopy of the “KK atoms” (i.e. their masses as a function of the quantum numbers associated with the internal dimensions) we can constrain the interactions of the KK modes with each others and with SM particles; this results in “selection rules” which control the decay of these modes. We focus on the AdS part of the geometry as an approximation of the actual KS throat. We employ standard (quantum mechanics) perturbation theory to compute the effect of the isometry breaking perturbations on the wave functions of the KK modes.

The interactions of the KK modes are studied in Section IV. We consider the model where the SM fields are localized on a 3-brane around the tip of the same throat where the excited KK modes are located. We study the possible decay channels of the long-lived modes and find that the leading one is into SM particles. This channel differs from the decay of scalar KK modes into massless gravi-vector particles which was recently considered in [27].

The second part of our paper is devoted to the consequences that the KK modes can have for cosmology and astrophysics. We first, in Section V, estimate the abundance of angular KK modes which freeze out in the hot expanding universe, and also estimate their life-times. We will mostly work with the conservative assumption of initial thermal equilibrium of KK modes.

It turns out that the theoretical predictions for the angular KK modes abundance and life-time are very strongly dependent on the parameters of the modes. Therefore, in Section VI we put together observational constraints on the parameters of KK modes and consequently, on the underlying throat model, using limits from BBN [29] and the astrophysical γ -ray background [31], in case of decaying modes, and limit on the dark matter energy density, in case of lifetimes much greater than the present age of the universe.

We restrict our calculations of the angular KK modes to single-throat settings. There are several reasons for that. The case of two throats, with one of them associated with (brane-antibrane) inflation (of energy scale 10^{13} GeV or so) and the other one associated with the standard model sector (of TeV energy scale), is often considered in the literature.

In the cosmological context, however, the story of KK modes in the two throat models with such significant energy offset has the following conceptual complication, which usually is not addressed in the literature. Indeed, first, the Hubble parameter scale $H \sim 10^{10}\text{GeV}$ of inflation exceeds the TeV mass of the SM throat KK modes. Similarly, the temperature T after brane-antibrane reheating exceeds that low mass scale. For those situations the low energy SM throat will be screened by a horizon². In other words, the KK mass spectrum of the low energy throat has a gap below defined by H or T . Therefore, the simple picture of KK modes tunneling from the inflationary throat to the SM throat is relevant only after the temperature of the universe drops below the TeV scale, i.e. when the timing of tunneling is longer than 10^{-12} sec. Another reason is that tunneling of the angular KK modes between the throats through the bulk of the inner manifold is exponentially suppressed.

In the Discussion Section we summarize our calculations and discuss generalizations of our results to other SM models and multiple-throat cases.

II. BACKGROUND WARPED GEOMETRY

In this section, we discuss the background geometry with the warped throat as a part of the inner space manifold. We will use this construction in the rest of the paper.

We consider a type IIB compactification with fluxes turned along the internal dimensions. A common feature of flux compactification is warping. The 10-D metric can be written

$$ds^2 = H^{-1/2}(z) g_{\mu\nu} dx^\mu dx^\nu + H^{1/2}(z) g_{ab}(z) dz^a dz^b, \quad (1)$$

or alternatively

$$ds^2 = e^{2A(y)} g_{\mu\nu} dx^\mu dx^\nu + \hat{g}_{ab}(y) dy^a dy^b. \quad (2)$$

The greek indices μ, ν, λ, \dots run over the 4-dimensional coordinates x^μ of the external space-time, while the latin indices a, b, c, \dots run over the 6-dimensional coordinates y^a of the internal compact space (whose metric is \hat{g}_{ab}). The outer space of the 10-dimensional background is approximated with the 4-dimensional Minkowski metric, $g_{\mu\nu} = \eta_{\mu\nu}$ ³.

² The emergence of the horizon in the KS throat was considered, e.g. in [30].

³ This approximation is poor when the Hubble parameter of the expanding universe exceeds the typical mass scale at the tip of the throat (like the masses of KK modes). In this case the tip of the throat would be screened from the rest of the compact manifold by an horizon and the KK mass spectrum would acquire a mass gap $\gtrsim H$. In this paper $H \ll m \sim T$.

The 10-dimensional geometry involves one or several “throats”, each of them on one side ends with a regular “tip”, and on the other side is smoothly glued to the bulk of the CY manifold ⁴. The known solutions for the throat, e.g. the KS solution, involve specific isometries and formally have a non-compact radial dimension. In order to get a sensible four-dimensional effective theory, the throat has to be glued to a compact CY which does not preserve these isometries. This results in deviations from the isometric KS solution, which are increasing as we approach the bulk of the CY. On the other hand, these isometry breaking perturbations are expected to be exponentially suppressed at the bottom of the throat.

In the following sub-section, we discuss in more details the geometry of the throat. In sub-section IIB, we consider the breaking of the isometries due to the compact CY. In sub-section IIC, we discuss the essential parameters of the model.

A. Isometric KS throat

The known example of analytical throat solution ending with a regular tip is given by the Klebanov-Strassler solution [3], where the warped throat contains a deformed conifold. The deformed conifold [45] is a 6-dimensional space defined in $\mathbb{C}^4 = \mathbb{R}^8$ by the quadric

$$\sum_{i=1}^4 z_i^2 = \varepsilon^2, \quad (3)$$

where z_i are four complex coordinates. Far from the origin $z_i = 0$, the deformation ε may be neglected and the space approaches a cone. Its base, given by the intersection of (3) with the sphere in \mathbb{C}^4 ,

$$\sum_{i=1}^4 |z_i|^2 = \text{constant}, \quad (4)$$

is the 5-dimensional manifold $T^{1,1}$, a fibration of $U(1)$ over $S^2 \times S^2$, which has the topology of $S^2 \times S^3$.

The warping is achieved by turning on M units of RR flux through a 3-cycle of the deformed conifold and $-K$ units of NS-NS flux through the dual 3-cycle. The full KS

⁴ The embedding geometry of the inner manifold reminds us of “an udder” with multiple tips sticking out. Baroque “udder” constructions are not so baroque for relativistic astrophysics: recall that the embedding diagram of the multiple supermassive black holes in the galaxies around us in an expanding universe also looks like an udder!

solution [3] involves rather tedious formula for the metric. Not all of its information will be needed for our discussion, therefore we will work with simpler approximations. Away from the bottom of the throat, the geometry is approximately given by the Klebanov-Tseytlin solution [4]

$$ds^2 = H^{-1/2}(r) \eta_{\mu\nu} dx^\mu dx^\nu + H^{1/2}(r) (dr^2 + r^2 ds_5^2) , \quad (5)$$

where ds_5^2 is the line element of $T^{1,1}$. The warping may be written

$$H(r) = \frac{R_+^4 + R_-^4 \ln\left(\frac{r}{R_+}\right)}{r^4} \quad (6)$$

with

$$R_+^4 = \frac{27\pi}{4} \alpha'^2 g_s M K \quad \text{and} \quad R_-^4 = \frac{81}{8} \alpha'^2 g_s^2 M^2 , \quad (7)$$

where $\sqrt{\alpha'}$ is the string length, g_s is the string coupling, and the amounts of fluxes M and K are chosen such that $R_+ > R_-$ (see Eq. (10) below). This approximate solution is valid only in the range $R_+ e^{-R_+^4/R_-^4+1} < r < R_+$. At smaller r , the singular metric based on the conifold has to be replaced by the regular one based on the deformed conifold [3]. At $r \sim R_+$, the geometry is glued to the compact CY.

Locally, the metric (5) corresponds to the direct product of AdS_5 and $T^{1,1}$ with the same radius of curvature R , but with $R^4 = R_+^4 + R_-^4 \ln\left(\frac{r}{R_+}\right)$ slowly (logarithmically) varying from $R = R_-$ to $R = R_+$. Taking R to be a constant between R_- and R_+ , the metric reduces to the simple form

$$ds^2 = e^{-2y/R} \eta_{\mu\nu} dx^\mu dx^\nu + dy^2 + R^2 f_{ij}(\Omega_5) d\theta^i d\theta^j , \quad (8)$$

where the coordinate $y = R \ln(R/r)$ measures the proper distance in the radial direction, and goes from $y = 0$ to $y = y_t$. f_{ij} is the metric on a 5-dimensional manifold X^5 , approximated by $T^{1,1}$ in the present case, and i, j, k, \dots run over the 5 ‘‘angular’’ coordinates θ^i (denoted collectively as Ω_5).

At the bottom of the KS throat (corresponding to $y > y_t$ in (8)), the $T^{1,1}$ evolves into a round S^3 of finite radius, while the two other angular directions, corresponding to the S^2 fibered over the S^3 , shrink to zero size. The geometry may be described in terms of a new radial coordinate ρ , with $r \propto e^{\rho/3}$ at large ρ . The asymptotic behavior of the metric in the vicinity of the tip at $\rho = 0$ reads as

$$ds^2 = e^{-2y_t/R} \eta_{\mu\nu} dx^\mu dx^\nu + R_-^2 [dS_3^2 + d\rho^2 + \rho^2 e_{ij}(\theta^k) d\theta^i d\theta^j] , \quad (9)$$

where the warp factor $e^{-2y_t/R}$ and the radius R_- of S^3 are approximately constant, and $e_{ij}(\theta^k)$ denotes the metric of the S^2 fibered over the S^3 . The total variation of the warp factor from the top to the bottom of the throat is approximately given by [1]

$$e^{-2y_t/R} \simeq e^{-\frac{2\pi K}{3g_s M}} , \quad (10)$$

which can generate naturally large hierarchies for suitable choices of fluxes.

The isometry group of $T^{1,1}$ is $SU(2) \times SU(2) \times U(1)$, as may be seen from its embedding (4) and (3) with $\varepsilon = 0$, where $SU(2) \times SU(2) \simeq SO(4)$ rotates the z_i 's and $U(1)$ multiply them by a phase. This is broken into $SO(4) \times \mathbb{Z}_2$ by the deformation ε of the conifold, where $SO(4)$ corresponds to rotations on the S^3 . These are the isometries of the KS throat.

B. Breaking Isometries by Gluing to CY

Kaluza-Klein modes in the 4 + 6 dimensional KS geometry with isometries in the angular dimensions carry angular momenta quantum numbers associated with them. Standard Model particles in the 4-dimensional outer spacetime do not have those quantum numbers. Therefore in an expanding universe excited angular KK modes will never be converted completely into the SM particles. In the model with isometric throat angular KK particles are the dangerous cosmological relics.

However, when the throat is glued to the compact CY at $y = 0$, its geometry deviates more and more from (8) as y decreases towards zero. In this sub-section we consider the background geometry of the throat which is smoothly glued to the big compact manifold. We will model this geometry as static perturbations around the isometric geometry (8). We write

$$ds^2 = e^{-2y/R} [1 + \epsilon(y) w(\Omega_5)] \eta_{\mu\nu} dx^\mu dx^\nu + dy^2 + R^2 [f_{ij}(\Omega_5) + \epsilon(y) \delta f_{ij}(\Omega_5)] d\theta^i d\theta^j , \quad (11)$$

where $\delta f_{ij}(\Omega_5)$ and $w(\Omega_5)$ are the isometry breaking perturbations at a given y of the metric on X_5 and of the warp factor respectively. For generic perturbations, only the 4-dimensional Lorentz invariance remains in (11). The perturbations are expected to be of order one at the base of the throat, where it is glued to the bulk of the CY, and to decrease exponentially away from it, $\epsilon(y) \sim e^{-\alpha y/R}$. In general, other supergravity fields and other components of the 10-dimensional metric may be perturbed as well, however, the form (11) will capture the effects we are interested in.

In principle, for a given throat model, the form of the isometry breaking perturbations may be calculated by harmonic analysis. The breaking of the $SO(4)$ isometry at the tip of the KS throat has been studied in [21] (see also [44]), where it was interpreted in the language of the AdS/CFT correspondence. From the point of view of the field theory dual to the warped background, the gluing of the compact CY to the throat may be described by the addition of symmetry breaking operators in the UV. The RG flow of these operators corresponds to the radial profile of the perturbations of the 10-dimensional background. On an $AdS_5 \times X^5$ background, a perturbation $\epsilon(y) \delta f_{ij}(\Omega_5)$ is decomposed into harmonics $\delta f_{ij}^{(L)}(\Omega_5)$ on X^5 , each with its own profile in the radial direction

$$\epsilon(y) \delta f_{ij}(\Omega_5) \rightarrow \sum_{\{L\}} e^{-\alpha_L y/R} \delta f_{ij}^{(L)}(\Omega_5) , \quad (12)$$

where we have neglected the sub-leading contributions with respect to y . The radial profile follows from the linearized radial mode equation after dimensional reduction on X^5 . The parameters α_L thus depend on the mode under consideration and its quantum numbers L on X^5 . The leading perturbation in the throat arises from the mode with the lowest value of α_L .

Ref. [21] classified the perturbations, breaking the $SO(4)$ isometry but preserving 4-dimensional Lorentz invariance and supersymmetry, which may be turned on a KS throat approximated by $AdS_5 \times T^{1,1}$. The leading perturbation found in [21] corresponds to a perturbation $e^{-\alpha_L y/R} \delta f_{ij}^{(L)}(\Omega_5)$ of the metric with $\alpha_L = \sqrt{28} - 4 \simeq 1.29$. It involves a tensor mode $\delta f_{ij}^{(L)}(\Omega_5)$ on $T^{1,1}$ with quantum numbers $L = (l_1 = 1, l_2 = 1, r = 0)$, where (l_1, l_2, r) are the principal quantum numbers associated to the $SU(2)_1 \times SU(2)_2 \times U(1)$ isometry of $T^{1,1}$ (see [22] for the KK spectroscopy of the type IIB supergravity fields on $AdS_5 \times T^{1,1}$). The isometry breaking perturbations involving other harmonics are exponentially suppressed in the throat compared to the leading one. Note also that, for a perturbation with given radial profile $e^{-\alpha_L y/R}$, the principal quantum numbers are fixed but the other ones (those which are not involved in the eigenvalues of the Laplacian on X^5) may vary since they do not appear in the radial mode equation.

Finally, Ref. [21] estimated the perturbation of the warp factor e^{2A} at the tip of the KS throat induced by the perturbation δf_{ij} . The leading correction was found to be of the order $\delta A(y_t) \sim e^{-\alpha y_t/R}$ with the same coefficient $\alpha \simeq 1.29$. This mode is absent on the $AdS_5 \times T^{1,1}$ background but should correspond to a linear perturbation around the full KS

solution. Again, we expect different harmonics in the angular directions to have different exponential suppressions at the tip of the throat. Because these modes arise from deviations of the KS solution from $AdS_5 \times T^{1,1}$, their radial profile in the throat may differ from $e^{-\alpha y/R}$. However, what will be important for us is their suppression at the tip, $\delta A(y_t) \sim e^{-\alpha y_t/R}$, and it will be convenient to keep the profile $e^{-\alpha y/R}$ in the throat to model this suppression. The perturbation of the metric in the angular directions and the perturbation of the warp factor will play similar roles in the following.

C. Parameters of the Warped Geometry

Here we discuss the basic parameters of the warped compactification, which will enter into the formulas for the cosmological abundance and decay time of KK modes. The cosmological constraints from the dangerous KK relics will be given in terms of these parameters.

One of the essential parameters will be the leading exponent α_L (for the KK modes with quantum numbers L) for the isometry breaking, entering in (11), (12). In addition to the parameters α , and to the string length $\sqrt{\alpha'}$ and coupling g_s , our treatment will involve essentially three other parameters: the (AdS) radius of curvature R in (8), the volume of the whole 6-dimensional internal space V_6 , and the warp factor at the bottom of the throat $e^{-y_t/R}$. We now recall useful relations between these parameters.

The volume V_6 is dominated by the “big” compact CY manifold, and it is always greater than the contribution of the throat alone, $V_6^{1/6} > R$. For instance, for the KS throat this implies $V_6 > \int_{\text{throat}} d^6 y \sqrt{\hat{g}} \simeq \text{Vol}(T^{1,1}) R_+^6 / 2 = 8\pi^3 R_+^6 / 27$. We will also take $R > \sqrt{\alpha'}$ in order to work in the supergravity approximation. In KS, $R > R_- > \sqrt{\alpha'}$ may be achieved by a suitable choice of fluxes, see Eq. (7).

The string length and V_6 are related through the value of the 4-dimensional Planck mass

$$M_{\text{Pl}}^2 = \frac{2V_6}{(2\pi)^7 g_s^2 \alpha'^4} . \quad (13)$$

We will take $g_s = 0.1$ in the estimations below.

The final parameter is the value of the warp factor at the bottom of the throat, $e^{-y_t/R}$. We will distinguish the short throat and the long throat, when this parameter is relatively big or relatively small, correspondingly. The short throat is associated with the warped brane inflation proposed in [6], and is often called the inflationary throat. In the original

model, the normalisation of the adiabatic density perturbations generated during inflation reads as

$$\delta_H \simeq 0.4 N_e^{5/6} \left(\frac{T_3}{M_{\text{Pl}}^4} \right)^{1/3} e^{-4y_t/3R} \simeq 2 \times 10^{-5} \quad (14)$$

at a number of e-foldings $N_e \approx 60$. Here $T_3 = [(2\pi)^3 g_s \alpha'^2]^{-1}$ is the tension of the $D3$, $\bar{D}3$ branes responsible for inflation. The original KKLMMT inflationary construction has been generalized by several models (e.g. [7, 9, 10, 11]) for which the parameters may be different. Eq. (14) will serve as a convenient reference value for a short throat.

The long throat is associated with the hierarchy between the string scale and the TeV (electroweak) scale à la Randall-Sundrum [5], if the Standard Model degrees of freedom are located on a brane around the tip of throat. In this case the warping is significant

$$e^{-y_t/R} \approx \frac{\text{TeV}}{M_s}, \quad (15)$$

where $M_s = 1/\sqrt{\alpha'}$. However, it does not mean that inflation cannot be associated with the long throat. The original KKLMMT throat slow roll inflation suffers from the η -problem due to the conformal coupling of the inflaton. It turns out that one still can obtain sufficient fast roll inflation with the conformal coupling, but only in the long throat [8]. For this case, the estimation (14) for the amplitude of the inflaton cosmological fluctuations is not applicable.

Both Eqs. (15) and (14) determine the value of the following specific combination of the parameters

$$\mathcal{N} \equiv \left(\frac{V_6^{1/6}}{\sqrt{\alpha'}} \right)^3 e^{y_t/R}. \quad (16)$$

We will thus use this combination in the calculations of the KK modes abundance and decay times.

For the short throat (14), using Eq. (13) with $g_s = 0.1$, Eq. (16) gives

$$\mathcal{N} \approx 5 \times 10^5 \quad (\text{short throat}). \quad (17)$$

In this case, significant warping ($e^{y_t/R} \gg 1$) requires at least $V_6^{1/6}/\sqrt{\alpha'} \ll 80$, and smaller values for $R/\sqrt{\alpha'}$ and $V_6^{1/6}/R$. For example, $V_6^{1/6} \approx 5\sqrt{\alpha'}$ leads to $e^{y_t/R} \approx 4 \times 10^3$.

For the long throat, using Eqs. (13) and (15), we have

$$\mathcal{N} \approx 10^{17} \quad (\text{long throat}). \quad (18)$$

III. SPIN 2 KALUZA-KLEIN MODES

Let us recall the energy cascade at the end of the brane-antibrane inflation [14]. Brane-antibrane annihilation through tachyon decay results in the production of massive closed string loops, which further decay into KK modes, interacting with each others, and with SM particles. Massive KK modes are localized at the bottom of the throat, while massless four-dimensional gravitons are not. There are various KK modes of the inner manifold with the throat(s) with fluxes, e.g. [23, 24]. We will be interested in the KK modes with angular degrees of freedom associated with inner dimensions. In the KK sector with angular momentum, bearing in mind cosmological applications, we shall be primarily concerned with the lightest modes localized at the bottom of the throat. Unfortunately, the mass spectrum of KK modes in the KS geometry is not known exactly but only up to the order of magnitude estimation $m \sim e^{-y_t/R}/R$.

At this point the study can go into different directions, depending on the choice of the prototype KK modes. The choice of [27], based on the extrapolation of the $AdS_5 \times T^{1,1}$ KK spectroscopy, is the massive scalar modes. However, to make these modes unstable, [27] introduced additional SUSY breaking operator, and the final decay products involve massless gravi-vector modes ⁵. There can be other subtleties: next-to-the-lightest modes may be forbidden to decay into the lightest modes, and their decay time directly into SM particles may be different. We will encounter these situations in our calculations below. Therefore, a comprehensive investigation shall include different possibilities.

In this paper, as a representative set of these KK modes, for economy and definiteness, we focus on the spin-2 fields in four-dimensions, and their decay into excitations of the SM brane located in the same throat. The dynamics of the spin-2 KK modes follows from the ten-dimensional linearized Einstein equation. Their wave equation depends only on the 10-dimensional background metric and is decoupled from the fluctuations of the matter sources. Our purpose is to calculate the abundance and lifetime of angular KK modes and make connection between cosmological constraints and parameters of the model. The

⁵ Ref. [27] does not deal with brane degrees of freedom, and does not address the decay channel of the gravi-vectors into the SM sector. There are also question about helicity conservation of their KK modes interactions, and question about the mass of their scalar mode (lightest one in the $AdS_5 \times T^{1,1}$ background) after compactification (for this mode, special care has to be taken with the boundary conditions on a slice of AdS , see [25, 26]) and after moduli stabilization.

methodology we develop in this paper can be extended for different KK modes and different phenomenological settings of their decays.

The spin-2 fields correspond to the symmetric transverse-traceless perturbation $h_{\mu\nu}$

$$g_{\mu\nu} = \eta_{\mu\nu} + h_{\mu\nu}(x^\lambda, y^c) \quad \text{with} \quad \eta^{\mu\lambda} \partial_\lambda h_{\mu\nu} = \eta^{\mu\nu} h_{\mu\nu} = 0 . \quad (19)$$

of the 10-dimensional metric (2).

The equations of motion for the KK modes (19) in the background geometry (2) are derived in the Appendix. The 4-dimensional Poincare invariance allows to solve by separation of variables

$$h_{\mu\nu}(x^\lambda, y^a) = \sum_m \Phi_m(y^a) \gamma_{\mu\nu}^{(m)}(x^\lambda) , \quad (20)$$

where $\gamma_{\mu\nu}^{(m)}(x)$ are the purely 4-dimensional spin-2 fields of mass m , satisfying

$$\square_{(4)} \gamma_{\mu\nu}^{(m)} = m^2 \gamma_{\mu\nu}^{(m)} \quad (21)$$

with $\square_{(4)} = \eta^{\mu\nu} \partial_\mu \partial_\nu$. The wave equation for the radial profile of the modes in the internal dimension may be written

$$- \hat{\nabla}_c \left(e^{4A} \hat{\nabla}^c \Phi_m \right) = m^2 e^{2A} \Phi_m , \quad (22)$$

where $\hat{\nabla}_c$ is the covariant derivative associated to the metric in the internal space, \hat{g}_{ab} in (2).

The spectrum and profile of the modes are mainly determined by the region where the warp factor e^{2A} varies exponentially. We will first consider the KK modes in the local isometric background (8). When isometries are broken according to (11), the metric perturbations are suppressed, $\epsilon(y) \sim e^{-\alpha y/R} \ll 1$, in the main part of the throat. We will solve the KK mode equation around this non-isometric background at linear order in ϵ , by using the standard techniques of quantum mechanics perturbation theory (sub-section III B).

A. KK Modes of Isometric Throat

To study the spin-2 KK modes around the local geometry (8), we may use the results of the Appendix with $e^{2A(y^c)} = e^{-2y/R}$ and $\hat{g}_{ab} dy^a dy^b = dy^2 + R^2 f_{ij} d\theta^i d\theta^j$. In this geometry, the mode equation (22) reads

$$- \frac{d}{dy} \left[e^{-4y/R} \frac{d\Phi_m}{dy} \right] - \frac{e^{-4y/R}}{R^2} \Delta_f \Phi_m = m^2 e^{-2y/R} \Phi_m , \quad (23)$$

where Δ_f denotes the Laplace operator associated with the metric $f_{ij}(\Omega_5)$ of the angular coordinates.

The background symmetries lead to the separation of variables

$$\Phi_m(y^c) = \psi_{nL}(y) Q_L^M(\Omega_5) \quad (24)$$

with

$$\Delta_f Q_L^M = -F^2(L) Q_L^M, \quad (25)$$

where L denotes collectively the quantum numbers involved in the eigenvalues $F^2(L)$ of Δ_f , and M the other ones. For instance, if f_{ij} is the metric of the 2-sphere, Q_L^M are the usual spherical harmonics Y_L^M and $F^2 = L(L+1)$, where L are positive integers and M are integers with $|M| \leq L$. For a Klebanov-Strassler throat, Q_L^M would be the harmonics associated to the angular dimensions of the deformed conifold.

Substituting (24) in Eq. (23) and using (25) gives the radial wave equation

$$-\frac{d}{dy} \left[e^{-4y/R} \frac{d\psi_{nL}}{dy} \right] + \frac{e^{-4y/R}}{R^2} F^2(L) \psi_{nL} = m_{nL}^2 e^{-2y/R} \psi_{nL}, \quad (26)$$

whose eigenfunctions ψ_{nL} and eigenvalues m_{nL}^2 will depend on the quantum number(s) L (through $F^2(L)$) and on a radial quantum number n . For the massive modes ($m^2 \neq 0$), the solution for the radial wave-function is

$$\psi_{nL}(y) = N_{nL} e^{2y/R} \left[J_\nu(m_{nL} R e^{y/R}) - B_{nL} Y_\nu(m_{nL} R e^{y/R}) \right], \quad \nu = \sqrt{4 + F^2(L)}, \quad (27)$$

where J_ν and Y_ν denote the Bessel functions of order ν of the first and second kind. The constant B_{nL} and the mass spectrum m_{nL} are determined by the boundary conditions, while the constant N_{nL} is fixed by the normalization condition. In general, KK modes are strongly localized at the bottom of the throat, $y = y_t$, and their masses are of the order $m \sim \frac{e^{-y_t/R}}{R}$ ⁶.

Boundary conditions may be obtained by matching the solution (27) to the solution for the modes at the base (at $y = 0$) and at the tip of the throat (at $y = y_t$). The effect of the CY on the boundary condition is difficult to model since we don't know the explicit metric of the gluing region. Here we will focus on the modes in the interval $0 \leq y \leq y_t$ and for

⁶ Some KK modes of mass $m \sim V_6^{-1/6}$ may be localized instead in the bulk of the CY, see e.g. [38]. We will not consider such modes here because for sufficient warping they are much heavier: $V_6^{-1/6} \gg e^{-y_t/R}/R$.

simplicity impose Neumann boundary conditions at both ends. To the order of magnitude we will be eventually interested in, we don't expect the results to be very sensitive to the particular form of the boundary conditions. The conditions $\psi'_{nL}(0) = \psi'_{nL}(y_t) = 0$ translate into two conditions for the B_{nL}

$$\begin{aligned} B_{nL} &= \frac{(\nu - 2) J_\nu(m_{nL}R) - m_{nL}R J_{\nu-1}(m_{nL}R)}{(\nu - 2) Y_\nu(m_{nL}R) - m_{nL}R Y_{\nu-1}(m_{nL}R)} \\ &= \frac{(\nu - 2) J_\nu(m_{nL}R e^{y_t/R}) - m_{nL}R e^{y_t/R} J_{\nu-1}(m_{nL}R e^{y_t/R})}{(\nu - 2) Y_\nu(m_{nL}R e^{y_t/R}) - m_{nL}R e^{y_t/R} Y_{\nu-1}(m_{nL}R e^{y_t/R})}. \end{aligned} \quad (28)$$

In the following, we will be interested in the lightest among massive KK modes, for which $mR \ll 1$. In this case, the first equation above implies $B_{nL} \ll 1$. More precisely, $B_{nL} \propto (mR)^2$ for $\nu = 2$ and $B_{nL} \propto (mR)^{2\nu}$ for $\nu > 2$. The second equation in (28) then reduces approximately to

$$(2 - \nu) J_\nu(\xi_{nL}) + \xi_{nL} J_{\nu-1}(\xi_{nL}) = 0, \quad (29)$$

which determines the spectrum of the KK eigenmasses. We have defined ξ_{nL} according to

$$m_{nL} = \frac{\xi_{nL}}{R} e^{-y_t/R}, \quad (30)$$

where $n = 1, 2, 3, \dots$ counts the successive roots of Eq. (29) for a given ν . The mass of the KK modes increases with n and with ν , i.e. with $F^2(L)$ in (25). For $\xi_{nL} \gg 1$ we find an analytical approximated solution (obtained by expanding the Bessel functions for large argument)

$$m_{nL} \simeq \pi \left(\frac{\nu}{2} + n + \frac{1}{4} \right) \frac{e^{-y_t/R}}{R}. \quad (31)$$

When the throat is approximated by a patch of $AdS_5 \times T^{1,1}$, we can use the eigenvalues of the Laplacian for the scalar harmonics (25) on $T^{1,1}$, see e.g. [32, 33, 34]. We have

$$F^2(L) = 6 \left(l_1(l_1 + 1) + l_2(l_2 + 1) - \frac{r^2}{8} \right), \quad (32)$$

where $L = (l_1, l_2, r)$ are the $SU(2)_1 \times SU(2)_2 \times U(1)$ principal quantum numbers, with l_1 and l_2 both integers or both half-integers, and with $r/2 \in \{-l_1, \dots, l_1\}$ and $r/2 \in \{-l_2, \dots, l_2\}$. In this case we can calculate the spin 2 mass spectrum of the angular KK modes. For illustration, we list in Table I the lightest massive states when the throat is approximated by a patch of $AdS_5 \times T^{1,1}$ with Neumann boundary conditions for the radial wave functions.

n	l_1	l_2	$ r $	$F^2(L)$	ξ_{nL}
1	0	0	0	0	3.83
1	1/2	1/2	1	33/4	5.45
1	1	0	0	12	5.98
1	0	1	0	12	5.98
2	0	0	0	0	7.02
1	1	1	2	21	7.04
1	1	1	0	24	7.35
1	3/2	1/2	1	105/4	7.57
1	1/2	3/2	1	105/4	7.57
1	3/2	3/2	3	153/4	8.63
2	1/2	1/2	1	33/4	8.92

TABLE I: Lightest massive spin 2 KK modes of the throat approximated by a patch of $AdS_5 \times T^{1,1}$ with Neumann boundary conditions for the radial wave functions.

They are tabulated according to their radial quantum number n and their angular quantum numbers l_1, l_2, r .

Now we compute the normalisation constant N_{nL} . The normalisation condition for each $\gamma_{\mu\nu}^{(m)}(x)$ in (20) to represent a canonically normalized spin-2 field from the 4-dimensional point of view is given in Eq. (107). We normalize the wavefunctions in the angular directions according to

$$\int d^5\Omega_5 Q_L^M(\Omega_5) Q_{L'}^{M'}(\Omega_5) = \delta_{LL'} \delta_{MM'} , \quad (33)$$

where $d\Omega_5 = d\theta^1 \dots d\theta^5 \sqrt{f}$ is the element of solid angle. Eq. (107) (here for $D = 10$) then gives

$$\frac{M_{10}^8 R^5}{4} \int_0^{yt} e^{-2y/R} \psi_{nL}(y) \psi_{n'L}(y) dy = \delta_{nn'} \quad (34)$$

for the radial profile of the modes, where $M_{10}^8 = \frac{2}{(2\pi)^7 g_s^2 \alpha'^4}$. In the range of masses we are interested in ($e^{-yt/R} < mR \ll 1$), this integral is dominated by the upper limit, where we

can neglect the term in $B_{nL} Y_\nu$. This gives

$$N_{nL} \simeq \frac{2\sqrt{2}}{M_{10}^4 R^3} \frac{e^{-yt/R}}{J_\nu(\xi_{nL})} \left(1 - \frac{F^2}{\xi_{nL}^2}\right)^{-1/2}, \quad (35)$$

see e.g. [36]. It is more convenient to rewrite this in terms of the 4-dimensional Planck mass, by using Eq. (108):

$$N_{nL} \simeq \frac{2\sqrt{2}}{M_{\text{Pl}}} \left(\frac{V_6}{R^6}\right)^{1/2} \frac{e^{-yt/R}}{J_\nu(\xi_{nL})}, \quad (36)$$

where we have also neglected the last term in parenthesis (which is approximately equal to one).

For the modes with angular momentum, the second term in (27) is comparable to the first one at $y = 0$ and becomes quickly negligible as y increases. Their normalized wave function is thus well approximated by

$$\psi(y) \simeq \frac{2\sqrt{2}}{M_{\text{Pl}}} \left(\frac{V_6}{R^6}\right)^{1/2} \frac{J_\nu(m_{nL} R e^{y/R})}{J_\nu(\xi_{nL})} \frac{e^{2y/R}}{e^{yt/R}}. \quad (37)$$

Finally, Eq. (26) has a solution with $m_{nL}^2 = 0$ if $F^2(L) = 0$. This mode, with zero mass and no angular momentum, is the usual 4-D graviton. Its wave function is constant in the extra dimensions and normalized to

$$\Phi_0 = \psi_{00} Q_0^0 = \frac{2}{M_{\text{Pl}}}, \quad (38)$$

see (109) (for this specific mode, the the leading contribution to the normalisation constant comes from the bulk of the CY).

B. KK Modes of the Throat with Isometry Breaking Perturbations

We now study the spin 2 KK modes in the background geometry (11), where the isometry breaking perturbations are suppressed by $\epsilon(y) = e^{-\alpha y/R}$ in the throat. The corresponding mode equation is given by Eq. (22) with $e^{2A(y^e)} = e^{-2y/R} [1 + \epsilon(y) w(\Omega_5)]$ and $\hat{g}_{ab} dy^a dy^b = dy^2 + R^2 [f_{ij}(\Omega_5) + \epsilon(y) \delta f_{ij}(\Omega_5)]$. The function $\epsilon(y)$ is much smaller than one in the throat itself and we can treat it as a perturbation. Up to first order with respect to ϵ , the mode equation may be written as

$$[H_0 + V] \Phi_m = m^2 e^{-2y/R} \Phi_m, \quad (39)$$

where

$$H_0 = -\frac{\partial}{\partial y} \left[e^{-4y/R} \frac{\partial}{\partial y} \right] - e^{-4y/R} \frac{\nabla_{(f)}^2}{R^2} \quad (40)$$

is the unperturbed operator involved in the LHS of the mode equation (23) for the isometric background, while

$$V = \epsilon w H_0 - e^{-4y/R} \frac{d\epsilon}{dy} \left(2w + \frac{1}{2} f^{kl} \delta f_{kl} \right) \frac{\partial}{\partial y} - \frac{e^{-4y/R}}{R^2} \epsilon \left[\partial_i \left(2w + \frac{1}{2} f^{kl} \delta f_{kl} \right) f^{ij} \partial_j - \frac{1}{\sqrt{f}} \partial_i \left(\sqrt{f} \delta f^{ij} \partial_j \right) \right] \quad (41)$$

is the perturbation operator encoding the effects of isometry breaking.

To solve for Eq. (39), we may follow the standard procedure of perturbation theory, by expanding the wave function Φ_m on the complete set $\psi_{nL}(y) Q_L^M(\Omega_5)$ of solutions of the unperturbed problem of the previous sub-section, and determine the coefficients of the expansion by using the orthonormal conditions (33, 34). We then define the matrix elements

$$V_{nLn'L'}^{MM'} = \int dy d\Omega_5 \psi_{nL}(y) Q_L^M(\Omega_5) V \psi_{n'L'}(y) Q_{L'}^{M'}(\Omega_5) \quad (42)$$

of the perturbation operator V in the basis $\{\psi_{nL} Q_L^M\}$. The eigenvalues at zeroth order in ϵ , i.e. the KK masses squared m_{nL}^2 in the isometric background, will typically be degenerate since in particular they do not depend on the quantum number(s) M of the harmonics $Q_L^M(\Omega_5)$. In this case, the correct wave functions at zeroth order are the linear combinations which diagonalize the matrix elements of degenerate states (see e.g. [37]): $V_{nLn'L'}^{MM'} = 0$ for $m_{nL} = m_{n'L'}$ and $(n, L, M) \neq (n', L', M')$. We will keep the notation $\psi_{nL} Q_L^M$ for these correct wave functions at zeroth order.

The KK modes' masses up to first order in ϵ are then given by

$$m_{nLM}^2 = m_{nL}^2 + \frac{1}{4} M_{10}^8 R^5 V_{nLnL}^{MM}, \quad (43)$$

where m_{nL} are the masses at zeroth order considered in the previous sub-section. In general, the breaking of the isometries removes the degeneracy. We will be specially interested in the wave functions of the KK modes when the isometries are broken. Up to first order in ϵ ,

they are given by ⁷

$$\Phi_{nL}^M(y, \Omega_5) = (1 + \mathcal{O}(\epsilon)) \psi_{nL}(y) Q_L^M(\Omega_5) + \frac{1}{4} \sum_{\substack{n', L', M' \\ m_{n'L'} \neq m_{nL}}} \frac{M_{10}^8 R^5 V_{n'L'nL}^{M'M}}{m_{nL}^2 - m_{n'L'}^2} \psi_{n'L'}(y) Q_{L'}^{M'}(\Omega_5) + \dots, \quad (45)$$

where the ellipses stand for similar contributions due to the matrix elements between degenerate states (see [37]).

Of course, there is still a zero mode 4-D graviton, with zero mass and constant wave function, in the absence of isometries in the internal space. Indeed for this mode, the corrections to the zeroth order mass and wave function vanish: $V_{nL00}^{M0} = 0$ because $\psi_{00} Q_0^0$ is constant.

Consider now the matrix elements $V_{n'L'nL}^{M'M}$ between two massive states. The contribution of the first term in (41) to (42) may be written

$$V_{n'L'nL}^{M'M} = m_{nL}^2 \int_0^{y_t} dy e^{-2y/R} \epsilon(y) \psi_{nL}(y) \psi_{n'L'}(y) \int d\Omega_5 w(\Omega_5) Q_L^M(\Omega_5) Q_{L'}^{M'}(\Omega_5) + \dots. \quad (46)$$

The other terms in (41) lead to similar contributions. The integrals over the angles determine the transitions allowed (i.e. the non-vanishing matrix elements), while the y -integral determine their amplitude.

In the following, we will need the amplitude of the matrix element between two light massive states ($m_{nL} \sim m_{n'L'} \sim e^{-y_t/R}/R \neq 0$) with non-zero angular momentum ($L, L' \neq 0$). Using the expression (37) for the ψ_{nL} and with the change of variables $u = m_{nL} R e^{y_t/R}$, the y -integral in (46) for a perturbation $\epsilon(y) = e^{-\alpha y/R}$ gives

$$\begin{aligned} & \int_0^{y_t} dy e^{-(2+\alpha)y_t/R} \psi_{nL}(y) \psi_{n'L'}(y) = \\ & = \frac{8}{M_{\text{Pl}}^2} \frac{V_6}{R^6} \frac{R \xi_{nL}^{\alpha-2} e^{-\alpha y_t/R}}{J_\nu(\xi_{nL}) J_{\nu'}(\xi_{n'L'})} \int_{\xi_{nL} e^{-y_t/R}}^{\xi_{nL}} du u^{1-\alpha} J_\nu(u) J_{\nu'}\left(\frac{\xi_{n'L'}}{\xi_{nL}} u\right) \approx \frac{e^{-\alpha y_t/R}}{M_{\text{Pl}}^2} \frac{V_6}{R^5}, \end{aligned} \quad (47)$$

where we have used (30) and $\xi_{nL} \sim \mathcal{O}(1)$ for the lightest modes. For $u \rightarrow 0$, $J_\nu(u) \propto u^\nu$, so

⁷ The matrix (42) is not symmetric, but one may derive the relation

$$V_{n'L'nL}^{M'M} - V_{nLn'L'}^{MM'} = (m_{n'L'}^2 - m_{nL}^2) \int dy d\Omega_5 e^{-2y/R} \epsilon \left(w + \frac{1}{2} f^{kl} \delta f_{kl} \right) \psi_{nL} Q_L^M \psi_{n'L'} Q_{L'}^{M'}. \quad (44)$$

From this it can be shown that the wave functions (45) satisfy the orthonormal conditions (107) at first order in ϵ , as they should. This fixes the constant in $\mathcal{O}(\epsilon)$ in the first term of (45), but its expression will not be important for what follows.

the u -integral does not depend on its lower limit for $\alpha < 2 + \nu + \nu'$.⁸ The integral is then mainly accumulated around its upper limit, leading to the last equality in (47).

Therefore, for the non-vanishing matrix elements $V_{n'L'nL}^{M'M}$ between two light massive modes with angular momentum, the component of the first order wave function Φ_{nL}^M in (45) along the zeroth order wave function $\psi_{n'L'} Q_{L'}^{M'}$ is given by

$$\begin{aligned} \Phi_{nL}^M(y, \Omega_5) &= \frac{1}{4} \frac{M_{10}^8 R^5 V_{n'L'nL}^{M'M}}{m_{nL}^2 - m_{n'L'}^2} \psi_{n'L'}(y) Q_{L'}^{M'}(\Omega_5) + \dots \\ &\approx \frac{e^{-(1+\alpha)y_t/R}}{M_{\text{Pl}}} \left(\frac{V_6}{R^6} \right)^{1/2} e^{2y/R} J_{\nu'}(m_{n'L'} R e^{y/R}) Q_{L'}^{M'}(\Omega_5) + \dots, \end{aligned} \quad (49)$$

where we have used (108) and (30), and keep the contribution of one of the terms in the sum (45). Note that the first order correction to the wave function is smaller than the wave function at zeroth order by a factor of $\epsilon(y_t)$ at any position in the radial coordinate y .

IV. INTERACTIONS OF KK MODES

In this Section, we will study interactions of the KK modes. We shall include 3-legs and 4-legs self-interactions of the KK modes. Most important for cosmology will be interactions of KK modes with the Standard Model particles. This will depend on the SM phenomenology in the string theory setting. Following [14], we will consider a simple model of KK modes interacting with the SM located on a 3-brane around the tip of the same throat. Notice that this model differs from what was considered in [27]. The cases where the Standard Model degrees of freedom are located in the bulk of the CY or in another throat are further constrained and will be discussed in the last, conclusion Section.

The decay times of angular KK modes due to isometry breaking are much longer than the time scales for their annihilations. It is convenient to call them as the “late” decays due to isometry breaking versus “early” decays and annihilations which are taking place without isometry breaking. Therefore, we consider first the “early” channels of KK interactions, for

⁸ For $\alpha > 2 + \nu + \nu'$, the u -integral diverges for $u \rightarrow 0$ and is then dominated by its lower limit, leading to

$$\int_0^{y_t} dy e^{-(2+\alpha)y_t/R} \psi_{nL}(y) \psi_{n'L'}(y) \approx \frac{e^{-(2+\nu+\nu')y_t/R}}{M_{\text{Pl}}^2} \frac{V_6}{R^5}. \quad (48)$$

This case may be covered by replacing α with $\text{Min}(\alpha, 2 + \nu + \nu')$ in Eq. (49).

which the isometry breaking of the throat can be neglected. At this level we will deal with KK modes with conserved angular momenta (of inner isometries).

We first compute the coupling constants for KK modes self-interactions in sub-section IV A. In sub-section IV B, we then compute the coupling constants for the KK modes interactions with the SM at the brane, again, with no isometry breaking from the CY. In both cases, we pay special attention to the selection rules to be satisfied. This will allow us to identify the long-living angular KK modes, which could pose cosmological problems. We then study in sub-section IV C the “late” decays of the long-lived KK modes induced by the isometry breaking perturbations.

A. Self-interactions of KK Modes without Isometry Breaking Perturbations

For the decays and annihilations of KK modes into themselves, the effective four-dimensional Lagrangian and coupling constants are obtained by substituting the perturbations (19) into the bulk action, expanding to third and fourth order in $h_{\mu\nu}$, and integrating over the internal coordinates. This is done in details in the Appendix for the general background (2), up to third order in $h_{\mu\nu}$.

Here we consider KK modes self-interactions which are already present in the throat geometry (8) without isometry breaking, i.e. at zeroth order *w.r.t.* the isometry breaking parameter $\epsilon(y)$.

We start with the decay of a KK mode of mass m and quantum numbers (n, L, M) into two lighter KK modes, of masses m' and m'' , and quantum numbers (n', L', M') and (n'', L'', M'') . The corresponding terms in the effective action have the form

$$\begin{aligned} \frac{M_{10}^8 R^5}{2} \int e^{-2y/R} \psi_{nL} \psi_{n'L'} \psi_{n''L''} dy \int Q_L^M Q_{L'}^{M'} Q_{L''}^{M''} d\Omega_5 \int \gamma_{\mu}^{(m)\nu} \partial_{\sigma} \gamma_{\nu\rho}^{(m)} \partial^{\sigma} \gamma_{(m)}^{\mu\rho} d^4x = \\ = \lambda_{3\text{KK}} \int \gamma_{\mu}^{(m)\nu} \partial_{\sigma} \gamma_{\nu\rho}^{(m)} \partial^{\sigma} \gamma_{(m)}^{\mu\rho} d^4x, \end{aligned} \quad (50)$$

where $d\Omega_5 = d\theta^1 \dots d\theta^5 \sqrt{f}$ is the element of solid angle in the angular dimensions X_5 . The expression above may be obtained by substituting (24) into (110) for the background (8). Here M_{10}^8 is the 10-dimensional Planck mass, which is related to the 4-dimensional Planck mass M_{Pl} and the total volume of the internal space V_6 through Eq. (108). With our choice of normalisation for the wave function in the internal space, the $\gamma_{\mu\nu}^{(m)}$ are canonically

normalized spin 2 fields, and $\lambda_{3\text{KK}}$ is the corresponding coupling constant. Eq. (50) allows us to calculate $\lambda_{3\text{KK}}$.

Let us consider the selection rules that follows from Eq. (50). The conservation of the 4-dimensional energy and momentum in the center of mass frame reads as

$$m = \sqrt{m'^2 + \mathbf{k}^2} + \sqrt{m''^2 + \mathbf{k}^2}, \quad (51)$$

which requires in particular $m > m' + m''$.

The integral over $d\Omega_5$ imposes angular momentum selection rules. By contrast, the warped background has no translation invariance in the radial direction y , so the y -integral does not impose the conservation of the total KK modes mass: m may be different from $m' + m''$, contrary to the case of extra dimensions with translation invariance. However, if one of the decay product is the massless graviton, $m'' = L'' = M'' = 0$, its wave function is constant in the internal space and drops out of the integrals over the inner dimensions. With (33), the y -integral then reduces to the orthogonality conditions (34), which implies $m = m'$. Furthermore, decay of KK modes is cascading into lighter and lighter KK states. However, if one of the decay product is the zero-mode graviton, $m'' = 0$, then $m = m'$ is required, as we just saw above and is shown more generally in the Appendix (see Eqs. (110) and (111)). Therefore, a massive KK mode ($m \neq 0$) cannot decay into two massless gravitons $m' = m'' = 0$ (this also was noticed in [15]). It is also obvious that a massive KK mode cannot decay into one massless graviton and another massive mode since the condition $m = m'$ leaves no phase space for this process. Therefore, a massive KK mode cannot decay by 3-legs interactions into one or two zero-mode graviton(s). As shown in the Appendix, this is independent of any isometries in the internal space. In addition, suppose m_0 is the mass of the lightest massive KK mode ($m_0 \neq 0$). Evidently, only the modes with $m > 2m_0$ can decay into two other massive modes. We thus conclude that the modes with $m \leq 2m_0$ cannot decay by 3-legs interactions into any other spin 2 modes (massive or massless).

Finally, in the presence of isometries, the conservation of the corresponding angular momentum imposes further selection rules. In particular, a mode with non-zero angular momentum ($L \neq 0$) cannot decay into modes with non-zero angular momentum only ($L' = L'' = 0$), which implies that the lightest modes with non-zero angular momentum cannot decay into any other KK mode.

For the allowed interactions between 3 massive KK modes, the effective 4-dimensional

coupling constant is obtained by substituting Eq. (37) into the *l.h.s* of Eq. (50), and performing the integrals over the internal coordinates. The y -integral is accumulated mostly around $y = y_t$, leading to

$$\lambda_{3\text{KK}} \approx \left(\frac{V_6}{R^6} \right)^{1/2} \frac{e^{y_t/R}}{M_{\text{Pl}}} , \quad (52)$$

where we have neglected numerical factors of order unity and used (108) to express M_{10}^8 in terms of M_{Pl} and V_6 .

The coupling constants for KK modes 4-legs interactions are obtained in the same way as we did it above for the 3-legs interactions. Expansion of the bulk action to the fourth order *w.r.t.* $h_{\mu\nu}$ gives the effective coupling constant for interactions between four KK modes

$$\lambda_{4\text{KK}} \approx M_{10}^8 R^5 \int_0^{y_t} e^{-2y/R} \psi_{nL} \psi_{n'L'} \psi_{n''L''} \psi_{n'''L'''} dy . \quad (53)$$

For four massive modes, the integral is again dominated by the contribution around its upper limit, leading to

$$\lambda_{4\text{KK}} \approx \left(\frac{V_6}{R^6} \right) \frac{e^{2y_t/R}}{M_{\text{Pl}}^2} . \quad (54)$$

It is worth noticing that this is about the square of (52), $\lambda_{4\text{KK}} \approx \lambda_{3\text{KK}}^2$.

B. KK-SM particles Interactions Without Isometry Breaking Perturbations

To obtain the coupling constants for the decays and annihilations of KK modes into SM brane degrees of freedom, we consider 4-dimensional fields located on a probe brane at $y^c = y_b^c$ in the geometry (2). One can start with the DBI action for the probe brane and use the decomposition of the DBI action for the perturbative field fluctuations. For simplicity, for a light scalar four-dimensional brane degree of freedom H , we have

$$\int d^D x \sqrt{-G_{(\text{ind})}} G_{(\text{ind})}^{\mu\nu} \partial_\mu H \partial_\nu H \delta^{(6)}(y^c - y_b^c) = \int d^4 x \sqrt{-g(y_b^c)} g^{\mu\nu}(y_b^c) \partial_\mu \hat{H} \partial_\nu \hat{H} , \quad (55)$$

where $G_{\mu\nu}^{\text{ind}} = e^{2A(y_b^c)} g_{\mu\nu}(y_b^c)$ is the induced metric on the brane located at $y^c = y_b^c$. To zeroth order in $h_{\mu\nu}$, the kinetic term is canonical for the normalized scalar field $\hat{H} = e^{A(y_b^c)} H$, that we have substituted in the r.h.s. of Eq. (55). The interaction term $h^{\mu\nu} \partial_\mu \hat{H} \partial_\nu \hat{H}$ is then obtained by substituting $g_{\mu\nu} = \eta_{\mu\nu} + h_{\mu\nu}$, where $h_{\mu\nu}$ are the spin 2 KK modes (19). Later on, we will consider the branching ratios for the KK modes decay into different Standard Model fields. For the moment we are only interested in the overall coupling constant, which can be estimated for the simplest case of a light scalar field.

Consider the decay of a KK mode with quantum numbers (n, L, M) in (24) into two lighter 3-brane scalar degrees of freedom, $\text{KK} \rightarrow \text{b b}$, following from (55). It involves the term

$$Q_L^M(\Omega_b) \psi_{nL}(y_b) \int d^4x \gamma_{(m)}^{\mu\nu} \partial_\mu \hat{H} \partial_\nu \hat{H} = \lambda_{\text{KKbb}} \int d^4x \gamma_{(m)}^{\mu\nu} \partial_\mu \hat{H} \partial_\nu \hat{H} , \quad (56)$$

where Ω_b and y_b denote the position of the brane in the angular and radial dimensions respectively.

At first glance, the coupling constant λ_{KKbb} somehow depends on the value of the angular eigenmode of the KK wave function at the position of the brane. While the brane will break some, but not all, the isometries of the bulk, the interaction (56) should respect the conservation of angular momentum associated with the remaining isometries.

To illustrate that the interaction in the form (56) indeed conserves quantum numbers associated to the isometries unbroken by the brane, we consider an example where the bulk involves an exact 2-sphere S^2 . The setup is shown in Fig. 1. The angular dependence of the KK mode wavefunction on S^2 is given by the usual spherical harmonics, $Q_L^M \propto Y_L^M(\theta, \phi)$. A 3-brane breaks the $SO(3)$ isometry of the S^2 into $SO(2)$. Choosing, for instance, the z -axis to point in the direction of the position of the brane on the S^2 (here the north pole, see Fig. 1), $\theta_b = 0$, the coupling constant in (56) is proportional to $\lambda_{\text{KKbb}} \propto Y_L^M(\theta_b = 0) \propto P_L^M(0)$ (where P_L^M are the associated Legendre polynomials [36]). Notice that this vanishes for all $M \neq 0$, see Fig. 1 (where M is the projection of the angular momentum along the z -axis). This means that only the modes with $M = 0$ can decay. The conservation of the quantum number M associated to the isometries unbroken by the brane forbids the modes with $M \neq 0$ to decay. Indeed, for these modes, the angular momentum vector has a component along the z -axis, and rotations around this axis are left invariant by the brane. Analogously, a 3-brane on the 3-sphere at the tip of a Klebanov-Strassler throat breaks the $SO(4)$ isometry into $SO(3)$, and KK modes with non-zero angular momentum associated with the remaining isometries cannot decay.

For the allowed interactions, the coupling constant λ_{KKbb} in (56) is obtained by evaluating the wave function (37) at the position of the brane, $y = y_b$. For the decay of a massive KK mode ($m_{nL} \neq 0$), this gives

$$\lambda_{\text{KKbb}} \approx \left(\frac{V_6}{R^6} \right)^{1/2} \frac{e^{(2y_b - y_t)/R}}{M_{\text{Pl}}} \frac{J_\nu(m R e^{y_b/R})}{J_\nu(m R e^{y_t/R})} . \quad (57)$$

Comparing with Eq. (52), we see that the 3-legs coupling of a KK mode with brane degrees

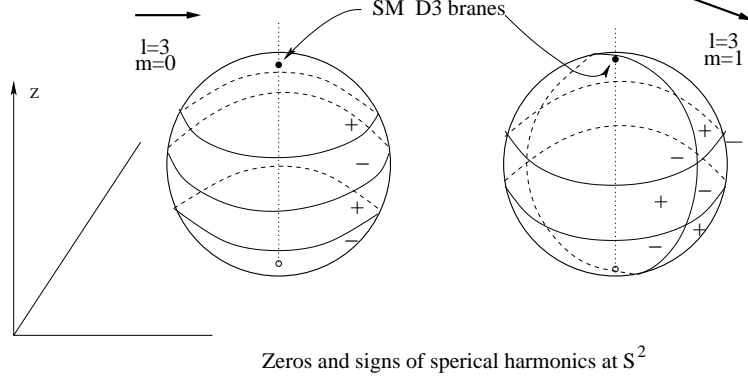


FIG. 1: Zeros and signs on the spherical harmonics on S^2 . We compare the $M = 0$ with the $M \neq 0$ case. The spherical harmonics with $M \neq 0$ vanish at the two poles. As a consequence, KK modes with nonvanishing angular momentum along the directions whose isometries are left unbroken by the brane are not directly coupled to brane fields (see the main text for details).

of freedom located at the tip of the throat, $y_b = y_t$, is of the same order as the 3-legs coupling of the KK modes between themselves. We will denote this coupling constant by λ_3 in the following

$$\lambda_{3KK} \approx \lambda_{KKbb} \approx \left(\frac{V_6}{R^6} \right)^{1/2} \frac{e^{y_t/R}}{M_{Pl}} \equiv \lambda_3 . \quad (58)$$

Interactions involving two KK modes and two brane degrees of freedom are obtained by expanding (55) to the second order in $h_{\mu\nu}$. The corresponding coupling constant is obtained in the same way as in (56). Again, it vanishes for KK modes with non-zero angular momentum associated with the isometries unbroken by the brane. For two other, massive KK modes, it is given by

$$\lambda_{KKKKbb} \approx \psi_{nL}(y_b) \psi_{n'L'}(y_b) \approx \left(\frac{V_6}{R^6} \right) \frac{e^{2(2y_b - y_t)/R}}{M_{Pl}^2} \frac{J_\nu(m R e^{y_b/R}) J_{\nu'}(m' R e^{y_b/R})}{J_\nu(\xi_{nL}) J_{\nu'}(\xi_{n'L'})} , \quad (59)$$

which again reduces to (54) when the brane degrees of freedom are located at the tip of the throat, $y_b = y_t$. We will denote this coupling constant by λ_4 , and it is related to λ_3 in (58) according to

$$\lambda_{4KK} \approx \lambda_{KKKKbb} \approx \lambda_3^2 \equiv \lambda_4 . \quad (60)$$

C. Late Decays of KK Modes due to Isometry Breaking Perturbations

In the isometric throat, the KK modes with non-zero angular momentum associated with the isometries unbroken by the brane (the modes with $M \neq 0$ in the S^2 example) cannot

decay into the brane degrees of freedom. Among these, the lightest ones cannot decay either into any other KK mode. They are therefore stable if the isometries are not broken, and become long-lived when the isometries are slightly broken. This is illustrated by the diagrams of Fig. 2.

We now study how these long lived modes may decay in the background (11), where the isometry breaking perturbations from the CY have radial profile $\epsilon(y) \ll 1$ in the throat. We proceed as in the previous sub-sections, but now we consider the effective action at first order in ϵ . The corresponding wave functions for the KK modes were calculated in sub-section III B.

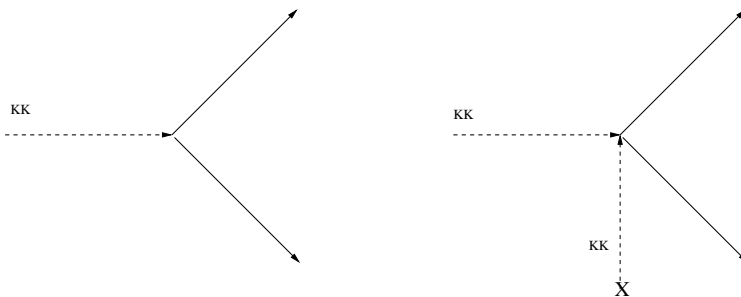


FIG. 2: Left panel: for the isometric throat, the decay of angular KK modes localized around the tip of the throat is forbidden by higher-dimensional angular momentum conservation. Right panel: The isometry breaking leads to a new interaction, which corresponds to the decay of an angular KK mode into SM particles mediated by a background isometry breaking KK mode localized in the compact CY.

Consider first the interactions between 3 KK modes described by (110). The corresponding 4-dimensional coupling constant at first order in ϵ includes terms involving the first order correction to e^{2A} and \sqrt{g} , and 3 zeroth order KK modes wave functions

$$\lambda_{3\text{KK}}^{(\epsilon)} = \int dy e^{-2y/R} \epsilon(y) \psi_{nL} \psi_{n'L'} \psi_{n''L''} \int d\Omega_5 \left(w + \frac{1}{2} f^{kl} \delta f_{kl} \right) Q_L^M Q_{L'}^{M'} Q_{L''}^{M''} + \dots \quad (61)$$

In addition, there are terms involving the unperturbed background metric and the first order ϵ correction to the wave-functions, not shown in (61). The complete expression is given by Eqs. (110) and (111).

In order to evaluate $\lambda_{3\text{KK}}^{(\epsilon)}$ it is sufficient to consider the first term in (61). There is, however, an exception. While the first term in (61) formally does not forbid to have massless $m = 0$ KK mode in that three-legs interaction, the total amplitude in this case is zero.

The reason is that the trilinear combination of the full KK wave functions in $\lambda_{3\text{KK}}^{(\epsilon)}$, when one of them is the constant zero-mode wave function, is effectively reduced to a bilinear combination. This bilinear combination is constrained by the orthonormality conditions of the full wave functions, which forbids the three-legs interactions involving one or two zero-mode(s). See the appendix for details ⁹.

In general, the isometry breaking perturbations are decomposed into harmonics $w^{(\mathcal{L})}(\Omega_5)$ and $f_{ij}^{(\mathcal{L})}(\Omega_5)$ with different quantum numbers \mathcal{L} , each with its own profile in the radial direction, see section II B and Eq. (12). Consider the selection rules resulting from a given harmonic $f_{ij}^{(\mathcal{L})}$ with radial profile $\epsilon(y) = e^{-\alpha_{\mathcal{L}}y/R}$ in (61) ¹⁰. The function $f^{kl}\delta f_{kl}^{(\mathcal{L})}$ in the integral over the angles breaks the conservation of angular momentum, which may facilitate the decay cascade of the angular KK modes. However, for the lightest of them, the relevant process is their decay into modes with zero angular momentum ($L' = L'' = 0$), which requires $\int d\Omega f^{kl}\delta f_{kl}^{(\mathcal{L})}Q_L^M \neq 0$. The perturbation $f^{kl}\delta f_{kl}^{(\mathcal{L})}$ having given principal quantum numbers \mathcal{L} , it allows only the modes with the same angular momentum, $L = \mathcal{L}$, to decay into two modes with zero angular momentum. The lightest modes with angular momentum would then decay through the perturbations carrying their own quantum numbers. These perturbations may be exponentially suppressed compared to the leading one, resulting in exponentially longer lifetimes. Furthermore, as in sub-section IV A, the decay of the modes with $m \leq 2m_0$ is still kinematically forbidden, since this does not depend on the isometries of the internal space (see the Appendix). As illustrated in Table 1, there may be several of these modes. Because of these restrictive selection rules, the leading decay channels for the long-lived modes will be into brane degrees of freedom.

For the decay channels which are made possible due to a given isometry breaking perturbation with radial profile $e^{-\alpha y/R}$ in the throat, the coupling constant $\lambda_{3\text{KK}}$ is calculated by

⁹ The decay channel studied in [27] involves such zero mass KK mode. The corresponding coupling constant was calculated there from a truncated expression involving only the unperturbed KK wave functions. As we noticed, a similar procedure in (61) leads to an incorrect result.

¹⁰ The leading perturbation $\delta f_{ij}^{(\mathcal{L})}$ (the one with the lowest $\alpha_{\mathcal{L}}$) on $AdS_5 \times T^{1,1}$ identified in [21] corresponds to a traceless tensor mode on $T^{1,1}$, for which $f^{kl}\delta f_{kl}^{(\mathcal{L})}$ vanishes. In this case, the contribution of the leading perturbation to $\lambda_{3\text{KK}}^{(\epsilon)}$ comes from the perturbed wave-function (through the last term in (41)) or from the perturbation of the warp factor, leading to similar results. Here we consider the contribution of another harmonic for illustration and keep $\alpha_{\mathcal{L}}$ arbitrary.

evaluating the y -integral in (61) as we did in (47). For 3 light massive KK modes, this gives

$$\lambda_{3\text{KK}}^{(\epsilon)} \approx \left(\frac{V_6}{R^6} \right)^{1/2} \frac{e^{(1-\alpha)yt/R}}{M_{\text{Pl}}} . \quad (62)$$

We consider now the decay of a KK mode into 2 brane degrees of freedom at first order in ϵ . We are interested in the long-lived KK modes, i.e. the lightest modes with non zero angular momentum associated to the isometries unbroken by the brane. As in (56), the corresponding coupling constant is just given by the wave function evaluated at the position of the brane in the internal space. This vanishes at zeroth order for the modes we are interested in, so we have to consider the first order corrections to the wave functions Φ_{nL}^M given in (45).

The decay occurs through the combined effect of isometry breaking due to the CY and isometry breaking due to the $D3$ (or $\bar{D}3$) brane. The resulting selection rules are less restrictive but more involved than for the decay into two KK modes with zero angular momentum. As an illustration, we return to the example of a 3-brane located at $\theta_b = 0$ on a 2-sphere ($Q_L^M = Y_L^M$). The modes which could not decay into brane degrees of freedom in the isometric case were the ones with non-vanishing quantum number M . In the series (45), all the terms involving $Y_L^{M'}$ with $M' \neq 0$ still vanish at the position of the brane. The 4-dimensional coupling constant is thus given by

$$\begin{aligned} \lambda_{\text{KKbb}}^{(\epsilon)} &= \Phi_{nL}^{M \neq 0}(y_b, \theta_b = 0) = \\ &= \frac{1}{4} \sum_{\substack{n', L' \\ m_{n'L'} \neq m_{nL}}} \frac{M_{10}^8 R^5}{m_{nL}^2 - m_{n'L'}^2} V_{n'L'nL}^{0M} \psi_{n'L'}(y_b) Y_{L'}^0(\theta_b = 0) + \dots \end{aligned} \quad (63)$$

This coupling constant is nonvanishing if the wave function $\Phi_{nL}^{M \neq 0}$ acquires a non-zero component along some harmonic $Y_{L'}^0$ due to the perturbation, i.e. if there exists some L' such that $V_{n'L'nL}^{0M} \neq 0$ for $M \neq 0$. Using (46), the contribution of the first term in (41) to this condition may be written

$$\int d\Omega_2 w Y_L^M Y_{L'}^0 \neq 0 \quad \text{for} \quad M \neq 0 . \quad (64)$$

Consider the contribution of the leading perturbation (the one which is the less suppressed at the tip of the throat) $w^{(\mathcal{L})}$ with given principal quantum numbers \mathcal{L} . In our 2-sphere example, we would have $w^{(\mathcal{L})} \propto \sum_{\mathcal{M}=-\mathcal{L}}^{\mathcal{L}} Y_{\mathcal{L}}^{\mathcal{M}}$. In this case, the Ω_2 -integral in (64) is nonvanishing if there exists an L' such that $|\mathcal{L} - L| \leq L' \leq \mathcal{L} + L$, and if there exists an \mathcal{M} such that

$\mathcal{M} = M$. The first condition can always be satisfied, while the second one requires $L \leq \mathcal{L}$. Thus in this case the KK modes can decay into SM (brane) degrees of freedom through the leading perturbation if their angular momentum is smaller than the one of the perturbation. On the other hand, the KK modes with greater angular momentum can cascade into KK modes with lower angular momentum already at zeroth order in the isometry breaking, if kinematically possible. Whether all the long-lived modes can decay this way is clearly very sensitive to the details of the actual KK spectrum. The remaining long-lived modes, if any, have to decay through a sub-leading isometry breaking perturbation, or at higher order in perturbation theory, resulting in an exponentially longer decay time.

The coupling constant (63) for the decay of a massive KK mode into two lighter brane degrees of freedom through an isometry breaking perturbation with radial profile $e^{-\alpha y/R}$ may be calculated with (49)

$$\lambda_{\text{KKbb}}^{(\epsilon)} \sim \left(\frac{V_6}{R^6} \right)^{1/2} \frac{e^{-(\alpha+1)y_t/R}}{M_{\text{Pl}}} e^{2y_b/R} J_{\nu'}(m_{n'L'} R e^{y_b/R}) . \quad (65)$$

In principle, we should sum over all the terms (n', L', M') with non-vanishing matrix element in (63), but the term with mass $m_{n'L'}$ closer to the mass m_{nL} of the decaying KK mode dominate. Again, (65) reduces to (62) when the brane is at the tip of the throat, $y_b = y_t$.

To summarize, we argue that the leading decay channels for the long-lived modes are the ones into SM brane degrees of freedom. However, the decay of different KK modes may have to be induced by different isometry breaking perturbations of the throat. Different isometry breaking perturbations, in turn, lead to different values of α in (65). Note also that throat models with different isometries than the KS throat would lead to different values of α . For these reasons in the following we will keep α as a free parameter. The value $\alpha \simeq 1.29$ for the leading perturbation considered in [21] and related to scalar metric perturbations (shown as the vertical, “background” leg at the right panel of Fig 2) will serve as a reference value. We will denote by $\lambda_3^{(\epsilon)}$ the coupling constant (65) when the brane is at the tip of the throat ($y_b = y_t$)

$$\lambda_3^{(\epsilon)} \equiv \left(\frac{V_6}{R^6} \right)^{1/2} \frac{e^{(1-\alpha)y_t/R}}{M_{\text{Pl}}} . \quad (66)$$

V. RELIC ABUNDANCES

In this Section we estimate the relic abundance of the KK modes. Reheating after brane/anti-brane inflation proceeds through several stages [14]. The brane/anti-brane system mostly annihilates into heavy closed strings. The closed strings very quickly decay into the lighter KK modes [14, 15]. The KK modes are significantly lighter than the closed strings, and hence they are relativistic when they are produced. They then interact among themselves and with the (lighter) SM degrees of freedom on the brane. We can neglect the small isometry breaking of the throat for such considerations. Then, the only KK modes directly coupled to brane fields are those with zero angular momentum along the directions whose isometries are left unbroken by the brane. For brevity, we denote such modes by KK_0 , and the other KK ones (those that are not directly coupled to the brane) by KK_L . Due to their different behavior, the two types of modes are studied separately in two Subsections V A and V B below.

From these interactions, one can obtain the relaxation time needed for the KK modes to reach thermal equilibrium. It has been estimated in [14, 15] that, for a short (inflationary) throat, the relaxation time is quicker than the decay of the KK modes into SM fields. The situation is more model dependent in the long throat case; in the example of a long throat considered here, we fix the parameter \mathcal{N} by requiring that the warp factor “generates” the electroweak scale at the tip of the throat, cf. Eq. (15). However, our discussion below is not constrained by any particular inflationary mechanism. For instance, it is possible that the SM fields are in the long throat, while the inflationary brane/anti-brane system is in another throat. In this case, the KK modes and the SM fields in the long throat are in thermal equilibrium only if the tunneling or the decay of the KK modes from the inflationary to the long throat is fast enough; this issue is still under investigation (notice, for example, that different conclusions on the transfer of this energy density have been reached in [15] and [28]). We will briefly discuss these issues in the last Section.

Our goal is to give a general discussion of the phenomenological limits due to the long lived KK_L modes. To keep the discussion as general as possible, motivated by the findings of [14, 15], in the following analysis we simply assume that the KK modes are in thermal equilibrium among themselves and with the SM fields at some given temperature T . In this way, their number density is independent on the history preceding the establishment

of the thermal equilibrium, and it is simply set by the freeze-out temperature at which the interactions changing their number go out of equilibrium. We show below that, in the region of parameter space of relevance for phenomenology, this freeze out temperature is typically significantly lower than the mass of the KK modes, so that their abundance is strongly Boltzmann suppressed. As we mentioned, it is an interesting and rather involved problem to estimate the initial number density of KK modes (produced by cascading decays of excited closed strings), and to figure out how far from thermal equilibrium the KK modes will be. If complete thermalization is not achieved, one should expect a higher number density for the KK modes, since the Boltzmann suppression will be reduced. For this reason, the phenomenological bounds that we will discuss below based on the assumption of initial thermal equilibrium should be considered as conservative ones.

A. KK_0 modes

Let us first study the KK_0 modes. We consider both three- and four-legs interactions with the brane fields. The trilinear interactions have the coupling λ_3 discussed in Eq. (58); it leads to the decay rate to gauge bosons V , (Dirac) fermions ψ , and the Higgs scalar H on the brane [42]

$$\Gamma_{\text{KK}_0 \rightarrow VV} = \frac{\lambda_3^2 m^3}{160 \pi} \quad , \quad \Gamma_{\text{KK}_0 \rightarrow \bar{\psi}\psi} = \frac{\lambda_3^2 m^3}{320 \pi} \quad , \quad \Gamma_{\text{KK}_0 \rightarrow HH} = \frac{\lambda_3^2 m^3}{960 \pi} \quad . \quad (67)$$

These expressions assume that the KK modes are much heavier than the particle they decay into, which is always a good approximation for the cases we are considering (see below). The complete expressions, with the kinematical factors included, can be found in [42]. The total decay rate is

$$\Gamma_{\text{KK}_0 \rightarrow bb} = \left[\frac{12}{160 \pi} + \frac{3 \times 6 + 3 + 3 \times 1/2}{320 \pi} + \frac{1}{960 \pi} \right] \lambda_3^2 m^3 \simeq 0.047 \lambda_3^2 m^3 \quad , \quad (68)$$

where b stands for the SM particles at the brane. For the inverse decay, we instead estimate

$$\Gamma_{bb \rightarrow \text{KK}_0} \sim 10^{-2} \lambda_3^2 N_b \quad , \quad (69)$$

where $N_b \sim 0.1 T^3$ is the number density of any relativistic species on the brane. This estimate is actually valid for temperatures T comparable or greater than the mass m of the KK modes. At lower temperatures, the rate has an additional $\exp(-m/T)$ suppression

since most of the light degrees of freedom are not energetic enough to create a KK_0 mode (see for instance the analogous process discussed in appendix B of [39]). Assuming that the energy density of the universe is dominated by the brane degrees of freedom (as we will see, this is certainly true at temperatures comparable and lower than the masses of the KK modes), we have the expansion rate

$$H = \frac{\rho^{1/2}}{\sqrt{3} M_p} \sim \frac{0.3 g_*^{1/2} T^2}{M_p}, \quad (70)$$

where g_* is the number of light degrees of freedom on the brane (we take $g_* \sim 100$, as it is the case for the standard model at high temperatures).

This leads to

$$\begin{aligned} \frac{\Gamma_{\text{KK}_0 \rightarrow bb}}{H} &\sim 0.17 \left(\frac{m}{T}\right)^2 \lambda_3^2 m M_p, \\ \frac{\Gamma_{bb \rightarrow \text{KK}_0}}{H} &\sim 0.003 \left(\frac{T}{m}\right) \lambda_3^2 m M_p, \quad T \gtrsim m. \end{aligned} \quad (71)$$

where ¹¹

$$\lambda_3^2 m M_p \simeq 220 \mathcal{N} \left(\frac{\xi_{nL}}{5}\right) \left(\frac{R}{\sqrt{\alpha'}}\right)^{-7}. \quad (72)$$

We see that both the decay and the inverse decay are effective (namely, $\Gamma > H$) when $T \simeq m$ if $R/\sqrt{\alpha'} \lesssim 11$ for the short throat case, and $R/\sqrt{\alpha'} \lesssim 250$ for the long throat case.

The four-legs interactions are proportional to the coupling constant $\lambda_4 = \lambda_3^2$ given in Eq. (60). It is instructive to compare the rates of the four- and three-legs interactions. For $T \gtrsim m$, we find ¹²

$$\begin{aligned} \frac{\Gamma_{\text{KK}_0 \text{KK}_0 \rightarrow bb}}{\Gamma_{\text{KK}_0 \rightarrow bb}} &\sim \frac{10^{-2} \lambda_4^2 T^2 N_{\text{KK}_0} g_*}{10^{-2} \lambda_3^2 m^3 g_*} \sim 0.5 \lambda_3^2 m^2 \left(\frac{T}{m}\right)^5, \quad T \gtrsim m, \\ \frac{\Gamma_{bb \rightarrow \text{KK}_0 \text{KK}_0}}{\Gamma_{bb \rightarrow \text{KK}_0}} &\sim \frac{10^{-2} \lambda_4^2 T^2 N_b}{10^{-2} \lambda_3^2 N_b} \sim \lambda_3^2 m^2 \left(\frac{T}{m}\right)^2, \quad T \gtrsim m, \end{aligned} \quad (73)$$

where

$$\lambda_3^2 m^2 \simeq 5 \times 10^4 \left(\frac{\xi_{nL}}{5}\right)^2 \left(\frac{R}{\sqrt{\alpha'}}\right)^{-8}. \quad (74)$$

¹¹ To obtain this quantity we have first used the expression (58) for λ_3 , (30) for the mass m of KK modes, and (13) for the ratio V_6/M_p^2 . The remaining parameters combine to give one power of \mathcal{N} , as defined in eq. (16). The coefficient ξ_{nL} , has been normalized to the typical value assumed by the lightest KK modes in the spectrum.

¹² For the $2 \rightarrow 2$ interactions, we assume that the s -wave process is unsuppressed; for the present scattering, we have actually computed the cross sections for the transverse–traceless helicity of the KK_0 modes. The cross section for the other helicities is increased by additional powers of (T/m) in the $T > m$ regime.

In general, the $2 \rightarrow 2$ scatterings dominate at high temperatures, and the moment at which the trilinear interactions become dominant depends on the value of $R/\sqrt{\alpha'}$. One can also check that, at the temperature $T \simeq m$, these rates are also greater than the expansion rate (70), for $R/\sqrt{\alpha'} \lesssim 6$ in the short throat case, and for $R/\sqrt{\alpha'} \lesssim 37$ in the long throat case. If this is the case, such interactions lead to thermal equilibrium between the KK_0 modes and the brane fields.

As the temperature drops below the mass of a KK_0 mode, both the ratios (73) acquire an $\exp(-m/T)$ suppression factor (in this first case this is due to the Boltzmann suppression of N_{KK_0} ; in the second case this is due to the fact that the interaction at the numerator produces one more heavy particle than the one at the denominator). Also the inverse decay is exponentially suppressed in this regime, as we have discussed above. Therefore, the only interaction that remains active in the nonrelativistic regime is the decay of the KK_0 , which quickly eliminates these modes.

B. KK_L modes

The decay rate of the angular KK_L modes into brane fields is suppressed by the small isometry breaking of the throat. The decay rate is still given by Eq. (68), but now the coupling λ_3 is given by Eq. (66). Assuming that the brane is at the tip of the throat ($y_b = y_t$), and using the relations (13), (16), and (30), we can rewrite the total rate normalized by the KK mass as

$$\frac{\Gamma_{\text{KK}_L \rightarrow bb}}{m} \simeq \frac{90 \xi_{nL}^2}{N^{2\alpha}} \left(\frac{\sqrt{\alpha'}}{R} \right)^{8-6\alpha} \left(\frac{V_6}{R^6} \right)^\alpha. \quad (75)$$

Let us now estimate the relic abundance of these modes. Under the assumption of isometric throat, the KK_L modes are not coupled to the brane fields. However, they interact with the KK_0 modes studied in the previous subsection. As long as the modes are relativistic,

we have ¹³

$$T \gtrsim m : \begin{cases} \Gamma_{\text{KK} \rightarrow \text{KKKK}} \sim 10^{-2} \lambda_3^2 m^3 \\ \Gamma_{\text{KKKK} \rightarrow \text{KK}} \sim 10^{-2} \lambda_3^2 N_{\text{KK}} \\ \Gamma_{\text{KKKK} \rightarrow \text{KKKK}} \sim 10^{-2} \lambda_4^2 N_{\text{KK}} T^2 . \end{cases} \quad (76)$$

We do not need to distinguish between KK_0 and KK_L modes in these estimates. Analogously to what we saw in the previous subsection, the $2 \rightarrow 2$ scatterings are typically the dominant interactions in the relativistic regime. Also in this case, the rate for such interactions is faster than the Hubble rate. Indeed

$$\frac{\Gamma_{\text{KKKK} \rightarrow \text{KKKK}}}{H} \sim 2 \times 10^4 \left(\frac{\xi_{nL}}{5} \right)^3 \mathcal{N} \left(\frac{R}{\sqrt{\alpha'}} \right)^{-15} \left(\frac{T}{m} \right)^3 , \quad T \gtrsim m , \quad (77)$$

which is greater than one for $T > m$ and for $R/\sqrt{\alpha'} \lesssim 4.6$ in the short throat case, and for $R/\sqrt{\alpha'} \lesssim 26$ in the long throat case. In the following, we assume that this is the case, so that also the KK_L modes are in thermal equilibrium with the brane fields in this regime.

These reactions slow down and eventually freeze out when the KK_L modes become non-relativistic. In this regime there are three relevant interactions that can potentially reduce the abundance of a KK_L mode. The first is a $2 \rightarrow 2$ scattering with brane degrees of freedom, mediated by a virtual KK_0 mode. The second is a $2 \rightarrow 2$ scattering into two KK_0 modes. The third is a $2 \rightarrow 1$ inverse decay, producing a KK_0 mode. Once formed, the KK_0 modes then quickly decay into the brane degrees of freedom (as we saw in the previous subsection). In all these cases, the two incoming KK_L modes must combine to produce a zero angular momentum (in the directions corresponding to the isometries unbroken by the brane). This is also the reason why a single KK_L mode cannot interact with KK_0 or the brane modes.

The rate for these interactions can be roughly estimated as

$$T \lesssim m : \begin{cases} \Gamma_{\text{KK}_L \text{KK}_{-L} \rightarrow bb} \sim 10^{-2} \lambda_3^4 N_{\text{KK}_L} m^2 g_* \\ \Gamma_{\text{KK}_L \text{KK}_{-L} \rightarrow \text{KK}_0 \text{KK}_0} \sim 10^{-2} \lambda_4^2 N_{\text{KK}_L} m^2 \\ \Gamma_{\text{KK}_L \text{KK}_{-L} \rightarrow \text{KK}_0} \sim 10^{-2} \lambda_3^2 N_{\text{KK}_L} , \quad \text{if sufficiently high momentum} \end{cases} \quad (78)$$

¹³ Also in this case, the estimate for the $2 \rightarrow 2$ scattering is given for the transverse-transpose helicity; scatterings between different helicities have higher powers of T/m .

Since $\lambda_4 \approx \lambda_3^2$, the first interaction dominates over the second one, due to the greater amount of available channels (this is certainly true for the lightest KK_L modes, so that there are few lighter KK_0 modes they can annihilate into; as we will see, the abundance of the heavier KK_L modes is anyhow suppressed relative to the lighter ones). The last process can in principle be faster but (due to kinematical reasons) it typically involves only a negligible amount of KK_L particles. The two incoming KK_L particles can inverse decay only into a heavier KK_0 species. More precisely, denoting by m_0 the mass of the KK_0 mode, and by m the one of the incoming KK_L particles of a given species, the momentum of the two particles in the center of mass frame is forced to be

$$k = \sqrt{\frac{m_0^2}{4} - m^2} . \quad (79)$$

As we saw, the masses of the KK modes are discretized in units of

$$\Delta m \sim \frac{\pi}{R} e^{-y_t/R} . \quad (80)$$

It may be possible that, for some special case, there is a KK_0 mode having a mass m_0 slightly greater but very close to $2m$. In general, however, the value in (79) will be of the order of Δm . For the lightest among the KK_L modes, $\Delta m \sim m$. In the nonrelativistic regime, the abundance of the KK_L mode that we are considering is Boltzmann suppressed. Most of such particles have momentum $k \sim T \ll m$. The inverse decay $\text{KK}_L \text{KK}_{-L} \rightarrow \text{KK}_0$ can only happen if, in the center of mass frame, the particles have the much higher momentum (79). So, only a very few of the KK_L modes will be able to perform the inverse decay. The remaining particles do not have enough energy, and can be depleted only through the first two interactions in (78).

For this reason, we neglect the effect of the inverse decay in the abundance of the lightest KK_L modes (in this, we differ from [15], where the suppression that we have just discussed was not considered). We therefore need to estimate the moment at which the first process in (78) freezes out. From this, we then obtain the relic abundance of the KK_L modes. In the nonrelativistic regime,

$$N_{\text{KK}_L} \simeq 5 \left(\frac{m T}{2\pi} \right)^{3/2} e^{-m/T} . \quad (81)$$

Using the expression (70) for the Hubble rate we find (see the previous subsection for more

details in obtaining the final estimate)

$$\begin{aligned} \frac{\Gamma_{\text{KK}_L \text{KK}_{-L} \rightarrow b\bar{b}}}{H} &\sim 0.1 \lambda_3^4 m^3 M_p \left(\frac{m}{T}\right)^{1/2} e^{-m/T} \\ &\sim 10^6 \mathcal{N} \left(\frac{\xi_{nL}}{5}\right)^3 \left(\frac{\sqrt{\alpha'}}{R}\right)^{15} \left(\frac{m}{T}\right)^{1/2} e^{-m/T}. \end{aligned} \quad (82)$$

Equalizing this to unity, one can estimate the freeze-out temperature T_f .

In Figure 3 we show the ratio of m/T when the scatterings go out of equilibrium in the case of parameters which are typical of either a short or a long throat. We also set a rough bound of $m/T \gtrsim 3$ for the nonrelativistic approximation for the KK modes to be valid [40]. For higher values of $R/\sqrt{\alpha'}$ the KK_L decouple while still relativistic, which results in a greater abundance (at even higher values of $R/\sqrt{\alpha'}$ we could have that the scattering of the KK modes are never in thermal equilibrium; the abundance of the KK particles then depends on the specific details of the reheating scenario; due to this strong model dependence, we do not consider such cases here).

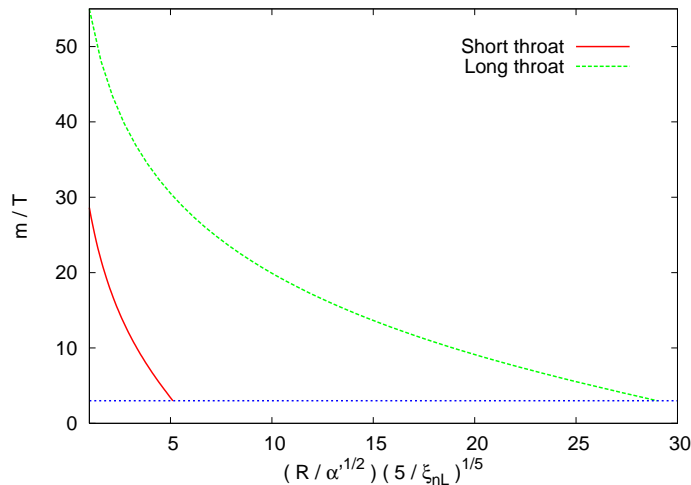


FIG. 3: Estimate for the m/T ratio at which the scatterings $\text{KK}_L + \text{KK}_{-L} \rightarrow b + \bar{b}$ freeze out. The value is strongly sensitive to the ratio $R/\sqrt{\alpha'}$.

Since this is the fastest interaction decreasing the number of KK_L , the moment at which this interaction freezes out sets the relic abundance of this species. In general, the later the freeze out occurs, the lower is the relic abundance of the mode (since the Boltzmann suppression is greater). From the horizontal axis of the Figure 3 we see that, for any fixed value of $R/\sqrt{\alpha'}$, the higher the mass of a KK_0 mode (greater ξ_{nL}), the higher is the value of m/T at which the freeze out occurs (later time). Therefore, the KK_L modes with higher

mass end up with a lower relic abundance. We show this in Figure 4, where we plot the ratio $Y_{\text{KK}_L} \equiv N_{\text{KK}_L}/s$ between the resulting number density N_{KK_L} and the entropy of the relativistic fields on the brane

$$s \simeq \frac{2\pi^2}{45} g_* T^3 \quad (83)$$

for the two cases $\xi_{nL} = 5, 10$. Also in this plot, we show only the cases for which the KK_L decouple while nonrelativistic.

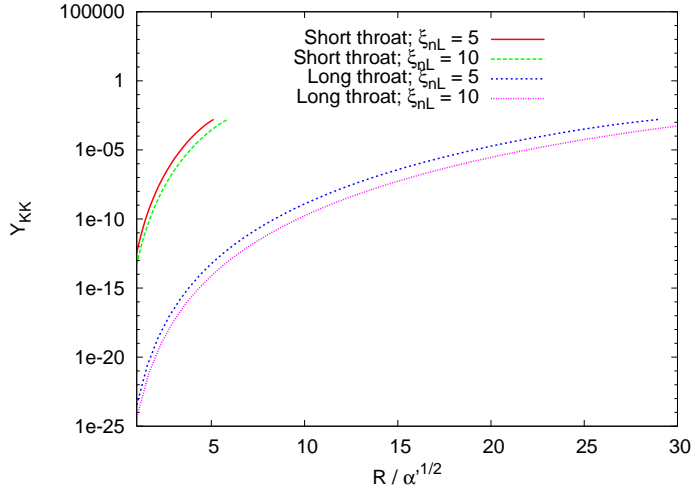


FIG. 4: Relic abundance for the KK_L species as function of parameter $R/\sqrt{\alpha'}$. We note that the lightest modes are more abundant than the heavier ones.

We can verify that the energy density of the KK_L modes is negligible with respect to that of the brane fields at the time at which they decouple (we used this assumption in setting the Hubble rate (70)). Since the KK_L are nonrelativistic, their energy density is simply their number density times their mass. For SM radiation (i.e. the light degrees of freedom on the brane), the energy density is instead related to the entropy density through $\rho = (3T/4)s$. This gives

$$\frac{\rho_{\text{KK}_L}}{\rho_{\text{rad}}} \simeq \frac{4}{3} \left(\frac{m}{T} \right) Y_{\text{KK}_L} \ll 1. \quad (84)$$

It is also worth noting that, for the specific case of warped brane/anti-brane inflation, the temperature after inflation is never higher than the mass of the KK modes. Indeed, even assuming that the thermalization occurs on a very quick timescale, the energy density during inflation, $\rho \simeq e^{-4yt/R}/(4\pi^3 g_s \alpha'^2)$, leads to a maximal reheating temperature $T_{\text{max}} \sim$

$0.23 e^{-y_t/R}/\sqrt{\alpha'}$. Using the expression (30) for the KK mass, we have

$$\frac{m}{T_{\max}} \sim 22 \left(\frac{\xi_{nL}}{5} \right) \left(\frac{\sqrt{\alpha'}}{R} \right). \quad (85)$$

As we can see in the Fig. 4, this value is comparable with the freeze-out temperature that we have obtained above. Therefore, our estimate for the number density is reliable in this case only if the thermalization is quick, as it appears from the estimates of the relaxation time given in [14, 15].

VI. PHENOMENOLOGICAL CONSTRAINTS

We are interested in the cosmological effects of the KK_L modes. Such modes are long-lived, since their decay rate is proportional to the small isometry breaking of the throat. We start by expressing the mass of the KK modes m_n in a more explicit form. By combining the three relations (13), (16), and (30), we can write

$$\frac{m_n}{M_p} \simeq \frac{44}{\mathcal{N}} \xi_{nL} \left(\frac{\sqrt{\alpha'}}{R} \right). \quad (86)$$

As we have seen in the previous Section, the lightest KK modes are in general those with the greatest abundance. Therefore, for definiteness, in the remainder of this analysis we consider only the presence of a single species with $\xi_{nL} = 5$, as it is typical for the lightest modes (stronger effects, and more stringent bounds, are obtained if more KK_L are generated with a comparable abundance). The typical values for \mathcal{N} are given in Eqs. (17) and (18). In the range of $R/\sqrt{\alpha'}$ considered in figures 3 and 4 above, we find

$$\begin{aligned} m &\sim (2 \times 10^{14} - 10^{15}) \text{ GeV} & , & \quad \text{short throat} \\ m &\sim (200 - 5,000) \text{ GeV} & , & \quad \text{long throat} \end{aligned} \quad (87)$$

As Eq. (84) shows, the KK_L particles dominate the energy density of the universe at sufficiently low temperature, provided they have not decayed before that. From the value of Y_{KK_L} shown in Fig 4, and from the expression (30) for the mass of the KK particles, we can find the temperature of the SM radiation, denoted by T_{dom} , at which the KK particles start to dominate¹⁴. The value T_{dom} as function of the parameters is shown in Figure 5; for

¹⁴ There is actually a slight difference in the value of g_* entering in the formula for the energy density and

comparison, we also show the value of the CMB temperature $T_{\text{eq}} \simeq 7.4 \cdot 10^{-10}$ GeV when matter starts to dominate in the universe ¹⁵.

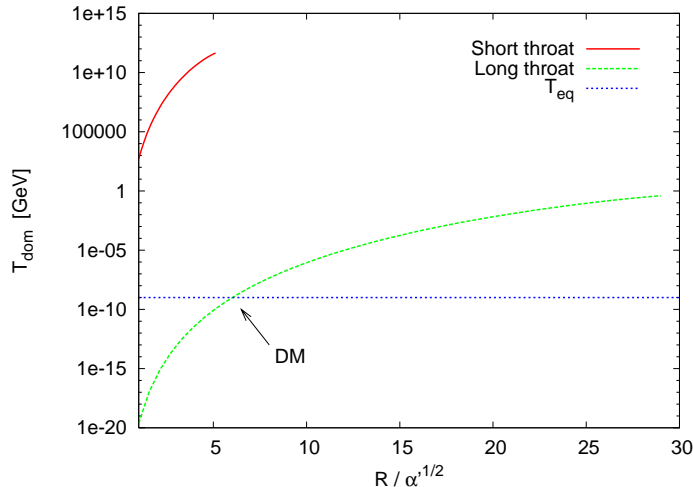


FIG. 5: Temperature of the universe at which the relic KK_L particles start to dominate, (provided they have not decayed yet) as function of $R/\sqrt{\alpha'}$. The temperature $T_{\text{eq}} \simeq 7.4 \cdot 10^{-10}$ GeV at the moment of matter–radiation equality is also shown for comparison. In the long throat, for $R/\sqrt{\alpha'} \simeq 6$, the KK modes can be the dark matter candidate.

Notice that intersection of two curves, T_{eq} and T_{dom} for the long throat selects the value of the parameter $R/\sqrt{\alpha'} \simeq 6$, in which case the KK modes can be the dark matter candidate. As we will see below, this also poses restrictions on the possible values of α . The Figure 5 will be discussed in details in the next two Subsections, where the two types of throats are studied separately.

A. Short throat

It is clear from Fig. 5 that, for the case of a short throat, it is phenomenologically required that all the KK_L modes decay. If this not the case, our universe would have become (and remained) matter dominated much before $z_{\text{eq}} \sim 10^4$, the redshift of matter-radiation equality, indicated by the observed values of Ω_m and of the CMB temperature (in other words, Ω_m

the entropy after e^\pm annihilation [40]. This introduces a factor 1.16 in Eq. (84) for $T \lesssim 0.5$ MeV. This effect is negligible at the level of accuracy of the present estimates.

¹⁵ Cosmological quantities in our universe are obtained by using the WMAP values $\Omega_\Lambda \simeq 0.73$, $\Omega_m \simeq 0.27$, $h \simeq 0.70$ [41].

today would be too big).

We therefore assume that the KK_L particles decay with the rate (75). We treat α as a free parameter. Typically, smaller values of α correspond to a greater break of isometry of the throat, and, consequently, to a quicker decay. From Eqs. (75) and (86), we find the lifetime of the angular KK modes

$$\tau \simeq \frac{1}{\Gamma_{\text{tot}}} \simeq 1.1 \times 10^{-27} \text{ s} \left(4 \times 10^3\right)^{2(\alpha-1.29)} \left(\frac{R}{5\sqrt{\alpha'}}\right)^{9-6\alpha} \left(\frac{R}{V_6^{1/6}}\right)^{6\alpha}. \quad (88)$$

We see that this lifetime is strongly dependent on the parameters of the model. For illustration, we show it in Figure 6 for a fixed value of $V_6^{1/6}/R$.

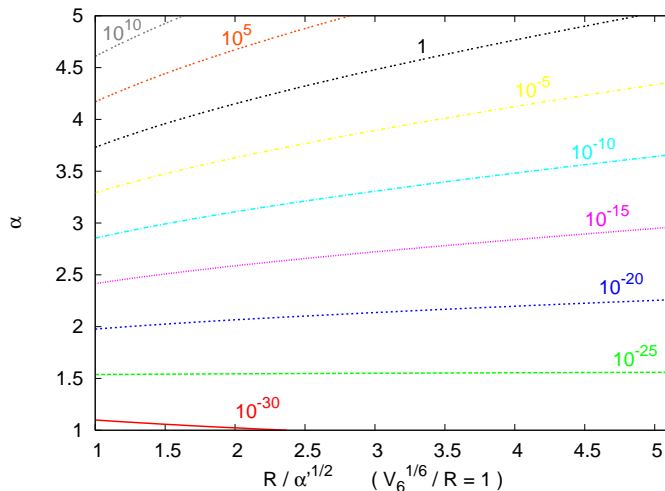


FIG. 6: Curves of lifetime (labelled by seconds) of the KK_L particles in the short throat case, as function of α and $R/\sqrt{\alpha'}$. For definiteness, we have fixed $V_6^{1/6}/R = 1$ in this plot. Higher values of this ratio correspond to a shorter lifetime, cf. Eq. (88).

Unless α is very high (very long lifetimes), the strongest phenomenological limits are those related to the effect that the decay products have on the abundance of light elements formed at Big-Bang Nucleosynthesis (BBN). Different limits are obtained for radiative and hadronic decays. KK_L have both type of decays, with $\mathcal{O}(1)$ branching ratios [42]. If we separate in Eq. (68) the rates into quarks and gluons from the other particles, we find a hadronic branching ratio of 0.73. Although the radiative decays are those which have been traditionally more studied, hadronic decays lead to stronger bounds. The BBN limits for a pure hadronic decay can be found in the Figures 38, 39, and 40 of [29]. These three figures present the constraints for decaying particles of mass $m = 100, 1,000, 10,000$ GeV,

respectively, in the $\tau - mY$ plane (for any given lifetime τ , there is an upper limit on the allowed values mY). The three cases do not show substantial differences from each other (at least, not at the level of accuracy of the present computation).

The limits of [29] have been approximately reproduced in our Fig. 10 below. We notice that the BBN limit is strongly relaxed and eventually disappears for lifetimes shorter than $\sim 10^{-2}$ s: if a particles decays before this time, the decay products thermalize before BBN starts. In our case, the product mY is an increasing function of $R/\sqrt{\alpha'}$, while it is independent of the other “free parameters” of the model ($V_6^{1/6}/R$ and α). For the values of $R/\sqrt{\alpha'}$ we are considering, mY ranges from ~ 400 GeV to $\sim 3 \times 10^{11}$ GeV. Such values are sufficiently high so that consistency with BBN requires that the decay took place place before $\sim 10^{-2}$ s¹⁶.

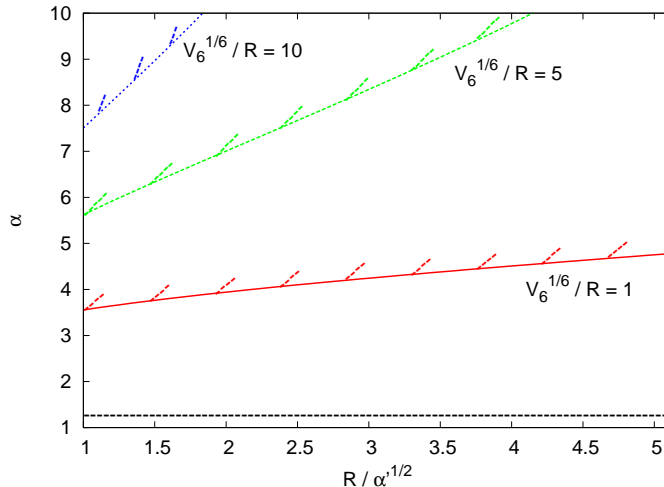


FIG. 7: BBN limit $\tau < 10^{-2}$ s for three reference values of the ratio $V_6^{1/6}/R$ for the short throat. For each case, regions above the lines (greater lifetime) are excluded. The horizontal line at $\alpha = 1.29$ corresponds to the reference value.

In Figure 7 we show the values of parameters leading to $\tau = 10^{-2}$ s. The three lines refer two three reference values of the ratio $V_6^{1/6}/R$. For each case, values above the lines shown result in a greater lifetime, and are therefore excluded.

It is possible that the KK_L particles dominate before decaying. This gives rise to an

¹⁶ It should be noted that the results of [29] have been obtained for much smaller masses than the typical KK masses for the short throat; nonetheless, we see that for all the masses considered in [29] (cf. their Figures 38, 39, and 40), the BBN bound disappear at $\tau \lesssim 10^{-2}$ s. For this reason, we take such value as a rough bound in the case of the higher injection energy considered here.

intermediate stage of matter domination. As long as this stage takes place before BBN, such a possibility is phenomenologically allowed¹⁷. To see whether this is the case, we compute the temperature of the thermal bath on the brane when the decay takes place; by equating the decay rate (75) (with the expression (86) for the mass) to the Hubble rate (70), we find

$$T_{\text{decay}} \simeq 2.2 \times 10^{10} \text{ GeV} (4 \times 10^3)^{1.29-\alpha} \left(\frac{100}{g_*}\right)^{1/4} \left(\frac{5\sqrt{\alpha'}}{R}\right)^{9/2-3\alpha} \left(\frac{V_6^{1/6}}{R}\right)^{3\alpha}. \quad (89)$$

In Fig. 5 above we showed the temperature T_{dom} of the brane at which the KK_L particles dominate, if they have not decayed yet. Therefore if the value of T_{decay} that we have just found is greater than the one of T_{dom} shown in that figure, the KK_L modes decay before dominating; the decay increases the temperature of the thermal bath by a negligible amount. If, on the contrary, $T_{\text{dom}} > T_{\text{decay}}$, the KK_L dominate the energy density of the universe when they decay. In this case, T_{decay} actually refers to the temperature of the thermal bath formed by the decay products¹⁸, which dominates over the pre-existing one on the brane.

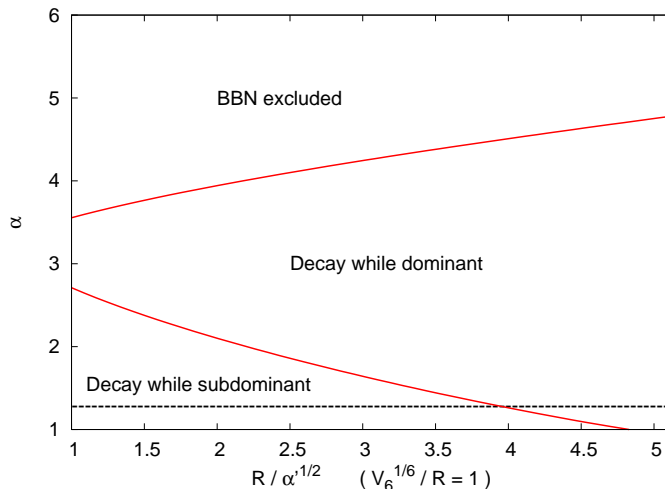


FIG. 8: Different scenarios for the decay of the KK_L particles in the short throat, for the fixed value $V_6^{1/6}/R = 1$. The horizontal line corresponds to the reference value $\alpha = 1.29$.

We show this effect in Figure 8, for the specific case of $V_6^{1/6}/R = 1$. The upper line is

¹⁷ Such stage can have interesting consequences for cosmology; for instance, it affects the relation between the wavelengths of observable cosmological perturbations and the moment when this mode leaves the horizon (efolds number) during inflation.

¹⁸ The thermalization of the decay products takes place on a much quicker timescale than the decay of the KK_L particles, and can therefore be considered as instantaneous for this discussion.

also shown in Fig. 7. Points above this line lead to a lifetime $> 10^{-2} \text{ s}$, and conflict with BBN bounds. For points in the intermediate region, the KK_L particles dominate the energy density of the universe when the decay. Prior to the decay, the universe is therefore matter dominated.

B. Long throat

Proceeding as in the previous Subsection, we now find the lifetime for the KK_L particles

$$\tau \simeq \frac{1}{\Gamma_{\text{tot}}} \simeq 3 \times 10^{13} \text{ s} (8 \times 10^{14})^{2(\alpha-1.29)} \left(\frac{R}{5\sqrt{\alpha'}} \right)^{9-6\alpha} \left(\frac{R}{V_6^{1/6}} \right)^{6\alpha}. \quad (90)$$

The lifetime is even more sensitive to the parameters of the model (particularly, to α) than in the previous case. For illustration, we show it in Figure 9 for the specific value $V_6^{1/6}/R = 10$ (as clear from Eq. (90), the lifetime is a decreasing function of this quantity). We see that the lifetime changes by several order of magnitudes in the range of value for α shown (notice that this range is smaller than the one shown in Fig. 6 for the short throat case).

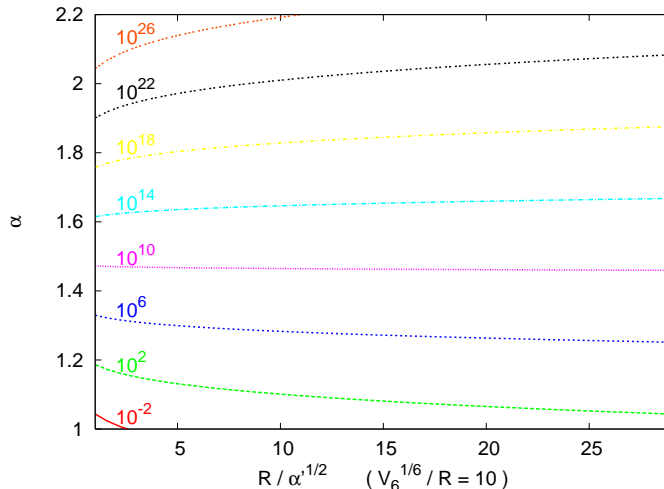


FIG. 9: Lifetime (in seconds) of the KK_L particles in the long throat. For definiteness, we have fixed $V_6^{1/6}/R = 10$ in this plot. Higher (shorter) values of this ratio correspond to a shorter (longer) lifetime, cf. Eq. (90).

We also observe that the lifetime of the modes can be easily comparable or much greater than the present age of the universe ($t_0 \simeq 4.3 \times 10^{17} \text{ s}$). The value of α at which the

two timescales are equal is only weakly (logarithmically) dependent on the other two “free parameters” of the model; for instance we find $\alpha \sim 1.4$ for $V_6^{1/6}/R = 1$, and for all the values of $R/\sqrt{\alpha'}$ considered in the long throat case; this is not much different than the value $\alpha \sim 1.8$ that can be seen in Fig. 9 for the $V_6^{1/6}/R = 10$ case. Due to the strong dependence of the lifetime on α , slightly higher values of this parameter result in a lifetime which is much longer than the present age of the universe.

In Figure 10 we show the phenomenological limits on an unstable particle of mass in the range (87) for the long throat case. Limits from BBN are taken from [29] (see the discussion in the previous subsection), while the ones from the diffuse γ ray background are taken from Fig. 12 of [31]. In both cases, the strongest limit comes from hadronic decays, which, for the KK_L particles, have a branching ratio of ~ 0.73 . In both cases, the phenomenological limits show a weak dependence on the mass of the particle in the interval of our interest; this dependence is negligible at the level of accuracy of the present analysis. We also show the limit obtained by requiring that the energy density of the KK_L particles is smaller than that of dark matter in our universe (this limit is relevant only for lifetimes greater than the present age of the universe).

Such limits have to be compared with the values of τ and of mY obtained for our model. For illustrative purposes, we also show in Fig. 10 the values obtained in the specific case of $V_6^{1/6}/R = 10$ (same choice as in Fig. 9). Each line shown corresponds to a given value of α , while $R/\sqrt{\alpha'}$ ranges in the interval $[1, 29]$ (that is, the usual one for the long throat case). As we already mentioned, the lifetime strongly increases with α .

The quantity mY only depends on $R/\sqrt{\alpha'}$, and it is a growing function of this ratio. Therefore, for any fixed values of the other “free parameters” of the model ($V_6^{1/6}/R$ and α), only values of $R/\sqrt{\alpha'}$ smaller than some given quantity are phenomenologically acceptable. We show this in Fig. 11. The three lines shown correspond to three reference values of $V_6^{1/6}/R$. For all the cases, the points on the right of the corresponding line are phenomenologically excluded. For values of $R/\sqrt{\alpha'}$ saturating this bound, the KK_L particles constitute the dark matter of our universe. In each case, the limit on $R/\sqrt{\alpha'}$ is strongest for an intermediate value of α ; this is the value for which the lifetime of the KK_L particles is comparable to the present age of the universe (we see in Fig. 10 that this is the point at which mY is most constrained). At higher values of α , the lifetime of the KK_L particles becomes much greater than the present age of the universe. In this case the only relevant

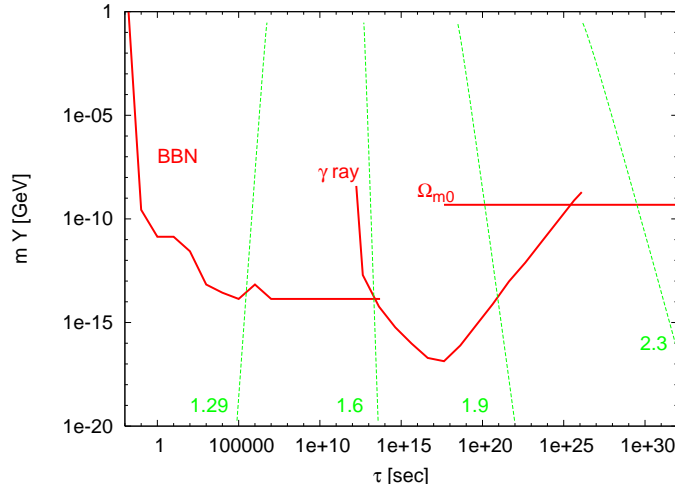


FIG. 10: Combined upper bound on the mass m times the abundance Y for an unstable particle with lifetime τ . The BBN limit is taken from [29], while the bound from the diffuse γ ray background from [31]. The horizontal line denoted by Ω_{m0} is the limit imposed by requiring that the energy density of the KK particle does not exceed the dark matter Ω . The other curves represent the values of τ and mY obtained in the long throat, for $V_6^{1/6}/R = 10$, for different values of α (indicated on the lines) and of $R/\sqrt{\alpha'}$ (mY is an increasing function of $R/\sqrt{\alpha'}$).

bound is that their energy density does not exceed the one of dark matter in the universe. Since the energy density depends only on $R/\sqrt{\alpha'}$, we find the same limit $R/\sqrt{\alpha'} \lesssim 6$ for all the values of α and $V_6^{1/6}/R$ in this range. When this limit is saturated, the KK modes are identified with the dark matter of the universe. On the contrary, for the lowest values of α shown, the modes decay before the onset of BBN, and the phenomenological limit disappears.

The “scaling” of the curves with $V_6^{1/6}/R$ shown in Figure 11 can be also easily understood. From Eq. (90), we see that the lifetime is a decreasing functions of $V_6^{1/6}/R$. This decrease is “compensated” by the growth of α in the numerical prefactor (which is by far the most sensitive quantity on α in that relation). Therefore, as $V_6^{1/6}/R$ increases, the same lifetime and the same “pattern” in the phenomenological limit is obtained by a small (logarithmic) increase of α). We see, in general, that for any given value of α , the decay can take place before BBN, provided the volume of the compact space is sufficiently large.

We conclude by commenting on the case in which the angular KK modes are identified with the dark matter of the universe. As we have already mentioned, the right abundance is obtained for $R/\sqrt{\alpha'} \simeq 6$. Moreover, limit from the diffuse γ ray background require that the lifetime of the modes is greater than about $3 \cdot 10^{25}$ s (cf. Fig. 10). The line in Figure 12

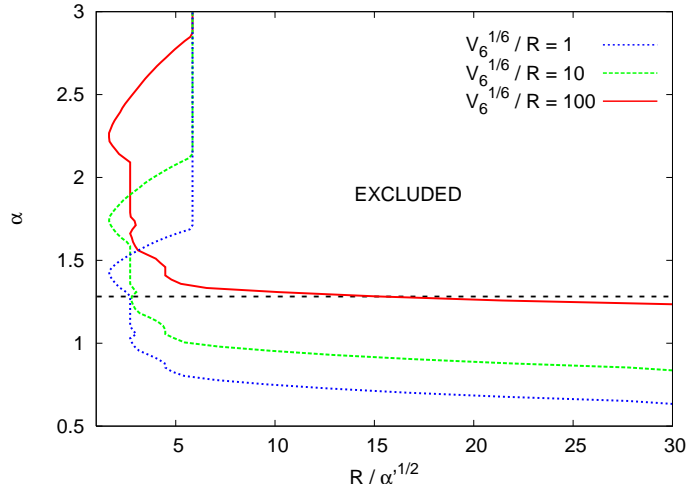


FIG. 11: Final exclusion region for the parameter in the long throat. The three lines correspond to three reference value of $V_6^{1/6}/R$. For each case, values of the parameters on the right of the corresponding curve conflict with the phenomenological limits shown in Fig. 10. The highest values of α shown result in KK_L particles with a much longer lifetime than the age of the universe. In this case, the only relevant bound is that the energy density of the KK_L particles does not exceed the one of dark matter in our universe. The horizontal line corresponds to $\alpha = 1.29$

represents the point in the $V_6^{1/6}/R - \alpha$ plane corresponding to this lifetime. Points below this line give a shorter lifetime, and are therefore phenomenologically excluded. In particular we see that $\alpha > 1.7$ is required for any value of $V_6^{1/6}/R > 1$. Therefore, the reference value $\alpha = 1.29$ does not allow to identify the angular KK modes with the dark matter of our universe.

VII. DISCUSSION AND CONCLUSION

In this paper, we have studied the problem of angular KK relics in string theory cosmology. As a specific example we considered angular KK modes resulting from approximate isometries of the internal space in the context of warped flux compactifications. We focused on the case where the isometries of the warped throat are distorted by its embedding into the compact manifold. The profile of the different isometry breaking perturbations of the throat (the parameters α_L in (12)) has been studied in [21] for a Klebanov-Strassler background, and we took their results as reference values.

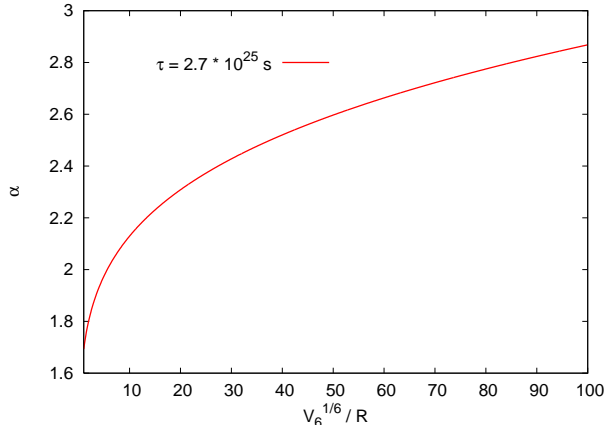


FIG. 12: Angular KK modes can be the dark matter candidate for $R/\sqrt{\alpha'} \simeq 6$ and for the values of the parameters α and $V_6^{1/6}/R$ above the line shown in the plot, corresponding to a lifetime of the KK particles greater than about $3 \cdot 10^{25}$ s (to avoid the limit from the diffuse γ ray background, cf. Fig. 10). For $V_6^{1/6}/R > 1$ this occurs for relatively large values of $\alpha > 1.7$.

We investigated the interactions and possible decay channels of the KK modes with angular momentum, calculating the corresponding coupling constants. We did explicit calculations for the spin 2 KK modes. We found that the lightest modes with angular momentum cannot decay directly into any other two KK modes (massive or massless), independently of the isometry breaking perturbations. We considered the model where the SM particles are localized on a (probe) 3-brane inside the throat. In this model the leading decay channel of the angular KK relics is the decay into brane degrees of freedom. Different KK modes may decay through isometry breaking perturbations with different exponents $e^{-\alpha y_t/R}$, resulting in exponentially different lifetimes. Our final expression for the lifetime of the relic KK modes then depends on several parameters: the degree of isometry breaking at the tip of the throat $e^{-\alpha y_t/R}$, the volume of the internal space V_6 , the AdS curvature radius R , and the throat warping $e^A = e^{-y_t/R}$. For completeness we also included as a parameter the position of the SM brane inside the throat $e^{-y_b/R}$.

We then studied the cosmological constraints on the parameters of the single throat model. We distinguished two limiting cases: a short throat where brane inflation occurs, and a long throat related to the hierarchy problem. In both cases, we considered the Standard Model fields to be located at the tip of the throat and to be at some moment in thermal equilibrium with the lightest KK modes. The freeze-out abundance of the KK relics then depends essentially on a single parameter ($R/\sqrt{\alpha'}$), although the dependance is very strong.

We considered the influence of the KK relics on the thermal history of the universe and put together observational constraints on the parameters of KK modes and consequently, on the underlying throat model, using limits from BBN [29] and the astrophysical γ -ray background [31], in the case of decaying modes, and limits on the dark matter energy density, in the case of lifetimes much greater than the present age of the universe. Such limits are very sensitive to the parameters of the models (see Fig. 7 for the short throat, and Fig. 11 for the long throat cases), but we can exhibit some general trends.

In the short throat, the lifetime of the KK relics is much shorter than in the long throat (since the warp factor is smaller and, consequently, physical times are quicker), but their relic abundance is also much higher. In this case, we must require that these modes decay before the onset of BBN, namely with a lifetime $\tau \lesssim 10^{-2}$ s. For greater lifetimes, the BBN and overclosure limits are typically exceeded by many orders of magnitude; therefore, the demand that the decay takes place before the onset of BBN holds even if the thermal history for the KK modes is slightly different than the one considered here (for instance, even if they do not reach perfect thermal equilibrium before they decay). We also showed that, for natural values of the parameters, the KK modes can dominate the energy density of the universe before decaying, see Fig. 8. This leads to an intermediate stage of matter domination in the early universe, which may have interesting consequences. For instance, it alters the thermal history of the universe, it affects the relation between the wavelength of present-day cosmological fluctuations and the corresponding number of e-folds of inflation, etc.

For the long throat case, a large fraction of the parameters space is excluded, see Fig. 11. In this case, for typical values of α obtained in [21] (such as $\alpha = 1.29$ for their leading isometry breaking perturbation), the constraints from the late decays require a sufficiently small value of $R/\sqrt{\alpha'}$ ($\lesssim 5$, or smaller), so that the abundance of the modes is strongly (Boltzmann) suppressed (recall that $R/\sqrt{\alpha'} \gtrsim 1$ is required for the validity of the supergravity treatment of the throat geometry). Otherwise, lower values of α , or a sufficiently large compact space ($V_6^{1/6}/R \gtrsim 100$), is required for these modes to decay before BBN. In the opposite regime, the lifetime of the KK relics can be much greater than the present age of the universe. If this is the case, or if, due to selection rules, some modes are stable, one gets the right abundance for these modes to be viable cold dark matter candidates if one tunes the value of $R/\sqrt{\alpha'} \simeq 6.1$. This also requires a value of $\alpha \gtrsim 1.7$.

In our analysis, we considered the Standard Model degrees of freedom to be located on a probe 3-brane at the tip of the throat where the KK modes are localized. The ultimate fate of the KK relics in a given model will depend on the specific way that the Standard Model is realized and embedded into the internal space. Furthermore, different or additional constraints may apply if the Standard Model degrees of freedom are located in the unwarped region of the Calabi-Yau or in another throat.

Already a displacement of the SM brane from the tip of the throat would affect the decay rate of the KK modes. In Sections 5 and 6, we only considered the probe brane to be at the tip, $y_b = y_t$. Otherwise ($y_b < y_t$), the decay time of the relic KK modes into SM particles would be much bigger, see Eq. (65). Shifting the SM brane from the tip has qualitatively similar effects than an increase of α , but quantitatively it is more involved. If $y_b < y_t$, all the KK modes interact much more weakly with the brane. In this case, even the modes with zero angular momentum can be dangerous relics, and observational constraints would be more stringent.

We restricted ourselves to the single throat case. The reason is related to at least two additional complications that arise if we include another throat. One complication arises for two throats with very different warpings. The physics of inflation and subsequent thermalization will correspond to values of the Hubble parameter and of the temperature which exceeds the mass of the KK modes in the long throat ($\sim TeV$). This generates a mass gap for the KK modes. The tunneling of KK modes from the short to long throat should take this effect into consideration. However, if the tunneling time is long enough to let the temperature drop below TeV scale, the usual treatment of tunneling may be consistent. The second complication is even more restrictive. Let us try to model the wave equation of the angular KK modes in the bulk space between throats [14]. Since warping there is insignificant, instead of equation (23) we have

$$\left(\partial_y^2 + m_{KK}^2 - \frac{p^2}{R^2}\right) \Phi_m = 0, \quad (91)$$

where we continue to use the “radial” coordinate y (in a loose sense) and where p^2 is the eigenvalue of the Laplace operator Δ_f in the directions orthogonal to y . Assuming that the angular momentum is connected to p^2 , we conclude that the angular KK modes are exponentially suppressed in the bulk, $\Phi_m \sim e^{-p(L)|y|/R}$. For $V_6^{1/6}/R \gg 1$ this effect exponentially suppresses the tunneling rate.

An interesting extension of the present analysis would be a more detailed study of the thermal history of the KK modes (or glueballs, in the dual theory), from their production by the decay of heavy closed strings formed after brane annihilation, to their thermalization among themselves and with light SM fields. In this work, we have conservatively assumed that complete thermalization is quickly achieved; this reduces significantly the abundance of the KK modes (due to Boltzmann suppression). One should expect the KK modes to have a much higher abundance if thermalization is not complete; this would lead to even stronger bounds on the parameters of the model than those obtained here.

We note the paper [46], which also made connection between cosmology and the glueballs in the dual picture of the gauge theory with extra isometries, which appeared as the present paper was being completed.

Acknowledgments

We thank Neil Barnaby, Alex Buchel, Igor Klebanov, Andrei Linde, Rob Myers, Keith A. Olive, Joe Polchinski, Sergey Prokushkin, Mikhail Voloshin and Piljin Yi for useful discussions. J.F.D. thanks CITA and the W.Fine Theoretical Physics Institute and the School of Physics and Astronomy of the University of Minnesota for their hospitality during different stages of this work. The work of J.F.D. was supported by CITA and by the Spanish MEC, via FPA2006-05807 and FPA2006-05423. The work of M.P. was partially supported by DOE grant DE-FG02-94ER-40823. Lev Kofman was supported by NSERC and CIFAR.

APPENDIX

In this Appendix, we derive the effective action to second and third order in the spin 2 KK modes (19) around the general background (2), assuming only 4-dimensional Lorentz invariance but independently of any isometries in the internal space. We then show that a massive mode cannot decay into one or two zero mode, generalizing a similar discussion in Section IV.

We consider the bulk action

$$S = \frac{M_D^{D-2}}{2} \int d^D x \sqrt{-G} (R + 2\mathcal{L}) , \quad (92)$$

where the lagrangian \mathcal{L} corresponds to all the matter in the bulk (scalar fields, forms, ...),

as well as possible brane localized sources. If the spacetime has boundaries, we should also add the appropriate Gibbons-Hawking boundary terms. The ansatz for the D -dimensional metric is

$$ds^2 = G_{MN} dx^M dx^N = e^{2A(y^c)} g_{\mu\nu}(x^\lambda, y^c) dx^\mu dx^\nu + \hat{g}_{ab}(y^c) dy^a dy^b, \quad (93)$$

where capital latin indices M, N, \dots run over the D -dimensional coordinates, greek indices μ, ν, λ, \dots run over the 4-dimensional coordinates, and latin indices a, b, c, \dots run over the internal $(D - 4)$ -dimensional coordinates of the compact space.

The background solution with 4-dimensional Lorentz symmetry corresponds to $g_{\mu\nu} = \eta_{\mu\nu}$ in (93). For the spin 2 perturbations, $g_{\mu\nu}$ will also depend on the coordinates x^μ and y^c , while the metric of the internal space \hat{g}_{ab} depends only on the extra-dimensions coordinates y^c .

Einstein equations are

$$R_{MN} = T_{MN} - \frac{T}{D-2} G_{MN} \quad \text{with} \quad T_{MN} = \mathcal{L} G_{MN} - 2 \frac{\delta \mathcal{L}}{\delta G^{MN}}, \quad (94)$$

where T is the trace of the energy-momentum tensor, $T = G^{MN} T_{MN}$. The background symmetries correspond to a matter lagrangian which is independent of the 4-dimensional metric: $\frac{\delta \mathcal{L}}{\delta g^{\mu\nu}} = 0$. The (μ, ν) and (a, b) components of Eq. (94) then read

$$R_{\mu\nu} = \frac{2}{D-2} \left(-\mathcal{L} + \hat{g}^{cd} \frac{\delta \mathcal{L}}{\delta \hat{g}^{cd}} \right) e^{2A} g_{\mu\nu}, \quad (95)$$

and

$$R_{ab} = \frac{2}{D-2} \left(-\mathcal{L} + \hat{g}^{cd} \frac{\delta \mathcal{L}}{\delta \hat{g}^{cd}} \right) \hat{g}_{ab} - 2 \frac{\delta \mathcal{L}}{\delta \hat{g}^{cd}}. \quad (96)$$

It is straightforward to compute the Ricci tensor of the metric (93). The (μ, ν) components are

$$\begin{aligned} R_{\mu\nu}[G] &= R_{\mu\nu}^{(4)}[g] - \frac{1}{2} \hat{\nabla}_c \hat{\nabla}^c (e^{2A} g_{\mu\nu}) \\ &\quad + \frac{1}{4} e^{-2A} g^{\lambda\rho} [2 \partial_c (e^{2A} g_{\mu\rho}) \partial^c (e^{2A} g_{\nu\lambda}) - \partial_c (e^{2A} g_{\lambda\rho}) \partial^c (e^{2A} g_{\mu\nu})] \end{aligned} \quad (97)$$

where $R_{\mu\nu}^{(4)}[g]$ is the 4-dimensional Ricci tensor of the metric $g_{\mu\nu}$, $\hat{\nabla}_a$ is the covariant derivative associated with the metric \hat{g}_{ab} , and a, b, c, \dots indices are raised and lowered with the metric \hat{g}_{ab} . Similarly, the (a, b) components of the D -dimensional Ricci tensor read

$$R_{ab}[G] = \hat{R}_{ab}[\hat{g}] - \frac{1}{2} \hat{\nabla}_a [e^{-2A} g^{\mu\nu} \partial_b (e^{2A} g_{\mu\nu})] - \frac{1}{4} e^{-4A} g^{\mu\nu} g^{\lambda\rho} \partial_a (e^{2A} g_{\mu\lambda}) \partial_b (e^{2A} g_{\nu\rho}) \quad (98)$$

where $\hat{R}_{ab}[\hat{g}]$ is the $(D - 4)$ -dimensional Ricci tensor of the metric \hat{g}_{ab} . To compute the effective action, we will also need the D -dimensional Ricci scalar for the ansatz (93). From Eqs. (97, 98), and performing the derivatives of the warp factor, we get

$$R[G] = e^{-2A} R^{(4)}[g] + \hat{R}[\hat{g}] + \frac{1}{4} g^{\mu\nu} g^{\lambda\rho} (\partial_c g_{\mu\rho} \partial^c g_{\nu\lambda} - \partial_c g_{\lambda\rho} \partial^c g_{\mu\nu}) - \frac{1}{2} \partial^c g^{\mu\nu} \partial_c g_{\mu\nu} - g^{\mu\nu} \hat{\nabla}_c \hat{\nabla}^c g_{\mu\nu} - \partial^c A (6g^{\mu\nu} \partial_c g_{\mu\nu} + g_{\mu\nu} \partial_c g^{\mu\nu}) - 8 \hat{\nabla}_c \hat{\nabla}^c A - 20 \partial_c A \partial^c A \quad (99)$$

where $R^{(4)}[g]$ and $\hat{R}[\hat{g}]$ are respectively the 4-dimensional and $(D - 4)$ -dimensional Ricci scalars of the metrics $g_{\mu\nu}$ and \hat{g}_{ab} .

We first consider the background solution, with $g_{\mu\nu} = \eta_{\mu\nu}$. Eq. (95) with (97) then gives

$$\hat{\nabla}_c \hat{\nabla}^c A + 4 \partial^c A \partial_c A = \frac{2}{D-2} \left(\mathcal{L} - \hat{g}^{cd} \frac{\delta \mathcal{L}}{\delta \hat{g}^{cd}} \right). \quad (100)$$

Similarly, contracting Eq. (96) with \hat{g}^{ab} and using Eq. (98) gives

$$\hat{R}[\hat{g}] + 2 \mathcal{L} = 6 \hat{\nabla}_c \hat{\nabla}^c A + 12 \partial_c A \partial^c A, \quad (101)$$

where we have used Eq. (100) to eliminate the term in $\hat{g}^{cd} \frac{\delta \mathcal{L}}{\delta \hat{g}^{cd}}$.

We now consider the spin 2 perturbations $h_{\mu\nu}(x, y)$, defined in (19). To obtain their effective action, we start from Eq. (92) with (99) and $\sqrt{-G} = \sqrt{\hat{g}} \sqrt{-g} e^{4A}$. We may then eliminate the background $(D - 4)$ -dimensional Ricci tensor $\hat{R}[\hat{g}]$ and matter lagrangian \mathcal{L} by using the relation (101). This gives

$$S = S_1 + S_2 \quad (102)$$

with

$$S_1 = \frac{M_D^{D-2}}{2} \int d^D x \sqrt{\hat{g}} \sqrt{-g} e^{2A} R^{(4)}[g] \quad (103)$$

and

$$S_2 = \frac{M_D^{D-2}}{2} \int d^D x \sqrt{\hat{g}} \sqrt{-g} e^{4A} \left[\frac{1}{4} g^{\mu\nu} g^{\lambda\rho} (\partial_c g_{\mu\rho} \partial^c g_{\nu\lambda} - \partial_c g_{\lambda\rho} \partial^c g_{\mu\nu}) - \frac{1}{2} \partial^c g^{\mu\nu} \partial_c g_{\mu\nu} - g^{\mu\nu} \hat{\nabla}_c \hat{\nabla}^c g_{\mu\nu} - \partial^c A (6g^{\mu\nu} \partial_c g_{\mu\nu} + g_{\mu\nu} \partial_c g^{\mu\nu}) - 2 \hat{\nabla}_c \hat{\nabla}^c A - 8 \partial_c A \partial^c A \right]. \quad (104)$$

We first expand the action to quadratic order in $h_{\mu\nu}$. After some integrations by parts (and neglecting the boundary terms), we can cast the action in the form

$$S^{(2)} = \frac{M_D^{D-2}}{8} \int d^D x \sqrt{\hat{g}} e^{2A} h^{\mu\nu} \left[\square_{(4)} + e^{2A} \left(\hat{\nabla}_c \hat{\nabla}^c h_{\mu\nu} + 4 \partial^c A \partial_c \right) \right] h_{\mu\nu}, \quad (105)$$

where greek indices are now raised and lowered with the 4-dimensional Minkowski metric $\eta_{\mu\nu}$ and $\square_{(4)} = \eta^{\mu\nu} \partial_\mu \partial_\nu$. The vanishing of the terms inside the brackets gives the equations of motion to first order in $h_{\mu\nu}$. With the separation of variables (20), this gives Eq. (22) for the profile of the modes in the internal space. The action (105) then becomes

$$S^{(2)} = \frac{M_D^{D-2}}{8} \sum_{m,m'} \int d^{D-4} y \sqrt{\hat{g}} e^{2A} \Phi_m \Phi_{m'} \int d^4 x \gamma^{\mu\nu(m')} [\square_{(4)} - m^2] \gamma_{\mu\nu}^{(m)}. \quad (106)$$

Therefore, with the orthonormal conditions

$$\frac{M_D^{D-2}}{4} \int d^{D-4} y \sqrt{\hat{g}} e^{2A} \Phi_m \Phi_{m'} = \delta_{mm'}, \quad (107)$$

the quadratic action decouples, and each $\gamma_{\mu\nu}^{(m)}$ represents from the 4-dimensional point of view a canonically normalized spin 2 field of mass m . For self-adjoint boundary conditions, the orthogonality conditions in (107) follows from the mode equation (22) in the usual way, by multiplying (22) by $\Phi_{m'}$, integrating by part over the internal space, and subtracting the equation obtained by interchanging m and m' .

Eq. (22) admits in particular a massless mode with a constant wave function in the internal space, $\Phi_0 = \text{constant}$. This mode represents the standard graviton in the 4-dimensional picture. The effective 4-dimensional Planck mass may then be obtained by performing the y -integral in (103) for a 4-dimensional metric $g_{\mu\nu}(x)$ depending only on the external coordinates

$$M_{\text{Pl}}^2 = M_D^{D-2} \int d^{D-4} y \sqrt{\hat{g}} e^{2A} = M_D^{D-2} V_{D-4}, \quad (108)$$

where V_{D-4} is the volume of the internal space. Using the normalisation (107), the wave function of the zero mode is then

$$\Phi_0 = \frac{2}{M_{\text{Pl}}}. \quad (109)$$

We now expand the action to third order in $h_{\mu\nu}$, in order to obtain the trilinear interactions between the spin 2 KK modes. For concreteness, we consider the decay of a mode of mass m into two modes of mass m' and m'' . The first term in (102, 103) gives contributions of the form

$$S_1^{(3)} \supset \frac{M_D^{D-2}}{2} \int d^{D-4} y \sqrt{\hat{g}} e^{2A} \Phi_m \Phi_{m'} \Phi_{m''} \int d^4 x \gamma_\mu^{(m)\nu} \partial_\sigma \gamma_{\nu\rho}^{(m')} \partial^\sigma \gamma^{(m'')\mu\rho}. \quad (110)$$

In general, the y -integrals do *not* require the conservation of the total KK mass, $m = m' + m''$, as would have been the case in a flat background. However, if one of the decay product is the

zero-mode, $m'' = 0$, its wave-function is constant and goes out of the integral. The y -integrals then reduce to the orthonormal conditions (107), which imposes $m = m'$. Therefore, a massive KK mode ($m \neq 0$) cannot decay into 2 zero modes gravitons ($m = m' = m''$), as also noticed in [15]. Here we note furthermore that a massive mode cannot decay either into another massive mode plus a graviton since, for the process $m \rightarrow m' + 0$, the constraint $m = m'$ is not compatible with the conservation of the 4-dimensional energy-momentum (51). We thus conclude that a massive KK mode cannot decay directly by 3-legs interaction into one or two zero-mode(s).

We can check that the second term in (102) does not change these conclusions. Expanding (104) to third order in $h_{\mu\nu}$ and performing integrations by part, we find after a tedious calculation

$$S_2^{(3)} = \frac{M_D^{D-2}}{2} \int d^D x \sqrt{\hat{g}} e^{4A} \left[\frac{1}{2} h^{\mu\nu} \partial_c h_{\nu\lambda} \partial^c h_\mu^\lambda - \partial^c A h^{\mu\nu} h_{\nu\lambda} \partial_c h_\mu^\lambda - \frac{1}{3} \left(\hat{\nabla}_c \hat{\nabla}^c A + 4 \partial_c A \partial^c A \right) h^{\mu\nu} h_{\nu\lambda} h_\mu^\lambda \right]. \quad (111)$$

We are interested in the contribution of this expression to the process $m \rightarrow m' + 0$. There is only one possibility for the constant zero-mode in the first term, 2 in the second term and 3 in the third term. The 4-dimensional coupling constant for this process is then proportional to

$$M_D^{D-2} \Phi_0 \int d^{D-4} y \sqrt{\hat{g}} e^{4A} \left[\frac{1}{2} \partial_c \Phi_m \partial^c \Phi_{m'} - \partial^c A \partial_c (\Phi_m \Phi_{m'}) - \left(\hat{\nabla}_c \hat{\nabla}^c A + 4 \partial_c A \partial^c A \right) \Phi_{m'} \Phi_m \right]. \quad (112)$$

By integrating the first and second terms by part, and by using the mode equation (22), this reduces to

$$\frac{M_D^{D-2}}{4} \Phi_0 (m^2 + m'^2) \int d^{D-4} y \sqrt{\hat{g}} e^{2A} \Phi_m \Phi_{m'}. \quad (113)$$

which again is non-vanishing only for $m = m'$, from the orthogonal conditions (107).

Therefore, the 3-legs decay of a massive spin 2 KK mode into 1 or 2 graviton zero-mode(s) is not possible. We will use this in Section IV when we study the possible decay channels of the KK modes.

-
- [1] S. B. Giddings, S. Kachru and J. Polchinski, Phys. Rev. D **66**, 106006 (2002) [arXiv:hep-th/0105097].
- [2] S. Kachru, R. Kallosh, A. Linde and S. P. Trivedi, Phys. Rev. D **68**, 046005 (2003) [arXiv:hep-th/0301240].
- [3] I. R. Klebanov and M. J. Strassler, JHEP **0008**, 052 (2000) [arXiv:hep-th/0007191].
- [4] I. R. Klebanov and A. A. Tseytlin, Nucl. Phys. B **578**, 123 (2000) [arXiv:hep-th/0002159].
- [5] L. Randall and R. Sundrum, Phys. Rev. Lett. **83**, 3370 (1999) [arXiv:hep-ph/9905221].
- [6] S. Kachru, R. Kallosh, A. Linde, J. M. Maldacena, L. McAllister and S. P. Trivedi, JCAP **0310**, 013 (2003) [arXiv:hep-th/0308055].
- [7] E. Silverstein and D. Tong, Phys. Rev. D **70**, 103505 (2004) [arXiv:hep-th/0310221] ; M. Alishahiha, E. Silverstein and D. Tong, Phys. Rev. D **70**, 123505 (2004) [arXiv:hep-th/0404084].
- [8] L. Kofman and S. Mukohyama, arXiv:0709.1952 [hep-th].
- [9] D. Baumann, A. Dymarsky, I. R. Klebanov, L. McAllister and P. J. Steinhardt, arXiv:0705.3837 [hep-th]; D. Baumann, A. Dymarsky, I. R. Klebanov and L. McAllister, arXiv:0706.0360 [hep-th].
- [10] A. Krause and E. Pajer, arXiv:0705.4682 [hep-th].
- [11] M. Becker, L. Leblond and S. E. Shandera, arXiv:0709.1170 [hep-th].
- [12] L. Kofman, A. D. Linde and A. A. Starobinsky, Phys. Rev. Lett. **73**, 3195 (1994) [arXiv:hep-th/9405187]; L. Kofman, A. D. Linde and A. A. Starobinsky, Phys. Rev. D **56**, 3258 (1997) [arXiv:hep-ph/9704452].
- [13] N. Barnaby, C. P. Burgess and J. M. Cline, JCAP **0504**, 007 (2005) [arXiv:hep-th/0412040].
- [14] L. Kofman and P. Yi, Phys. Rev. D **72**, 106001 (2005) [arXiv:hep-th/0507257].
- [15] X. Chen and S. H. Tye, JCAP **0606**, 011 (2006) [arXiv:hep-th/0602136].
- [16] A. R. Frey, A. Mazumdar and R. Myers, Phys. Rev. D **73**, 026003 (2006) [arXiv:hep-th/0508139].
- [17] D. Chialva, G. Shiu and B. Underwood, JHEP **0601**, 014 (2006) [arXiv:hep-th/0508229].
- [18] A. Butti, M. Grana, R. Minasian, M. Petrini and A. Zaffaroni, JHEP **0503**, 069 (2005) [arXiv:hep-th/0412187].
- [19] G. Servant and T. M. P. Tait, Nucl. Phys. B **650**, 391 (2003) [arXiv:hep-ph/0206071]

- ; H. C. Cheng, J. L. Feng and K. T. Matchev, Phys. Rev. Lett. **89**, 211301 (2002) [arXiv:hep-ph/0207125].
- [20] E. W. Kolb and R. Slansky, Phys. Lett. B **135**, 378 (1984).
- [21] O. Aharony, Y. E. Antebi and M. Berkooz, Phys. Rev. D **72**, 106009 (2005) [arXiv:hep-th/0508080].
- [22] A. Ceresole, G. Dall'Agata and R. D'Auria, JHEP **9911**, 009 (1999) [arXiv:hep-th/9907216].
- [23] S. B. Giddings and A. Maharana, Phys. Rev. D **73**, 126003 (2006) [arXiv:hep-th/0507158].
- [24] S. S. Gubser, C. P. Herzog and I. R. Klebanov, JHEP **0409**, 036 (2004) [arXiv:hep-th/0405282]; S. S. Gubser, C. P. Herzog and I. R. Klebanov, Comptes Rendus Physique **5**, 1031 (2004) [arXiv:hep-th/0409186].
- [25] A. Delgado and M. Redi, Phys. Lett. B **562**, 127 (2003) [arXiv:hep-th/0301151].
- [26] T. Gherghetta and A. Pomarol, Nucl. Phys. B **586**, 141 (2000) [arXiv:hep-ph/0003129].
- [27] A. Berndsen, J. M. Cline and H. Stoica, arXiv:0710.1299 [hep-th].
- [28] B. v. Harling, A. Hebecker and T. Noguchi, JHEP **0711**, 042 (2007) [arXiv:0705.3648 [hep-th]].
- [29] M. Kawasaki, K. Kohri and T. Moroi, Phys. Rev. D **71**, 083502 (2005) [arXiv:astro-ph/0408426].
- [30] A. Buchel, Nucl. Phys. B **600**, 219 (2001) [arXiv:hep-th/0011146]; S. S. Gubser, C. P. Herzog, I. R. Klebanov and A. A. Tseytlin, JHEP **0105**, 028 (2001) [arXiv:hep-th/0102172].
- [31] G. D. Kribs and I. Z. Rothstein, Phys. Rev. D **55**, 4435 (1997) [Erratum-ibid. D **56**, 1822 (1997)] [arXiv:hep-ph/9610468].
- [32] S. S. Gubser, Phys. Rev. D **59**, 025006 (1999) [arXiv:hep-th/9807164].
- [33] D. P. Jatkar and S. Randjbar-Daemi, Phys. Lett. B **460**, 281 (1999) [arXiv:hep-th/9904187].
- [34] D. Baumann, A. Dymarsky, I. R. Klebanov, J. M. Maldacena, L. P. McAllister and A. Murugan, JHEP **0611**, 031 (2006) [arXiv:hep-th/0607050].
- [35] L. Randall and R. Sundrum, Phys. Rev. Lett. **83**, 4690 (1999) [arXiv:hep-th/9906064].
- [36] M. Abramowitz, I. Stegun, *Handbook of Mathematical Functions*, Dover Publications (1973).
- [37] L. Landau, E. Lifshitz, Vol. III. *Quantum Mechanics: non-relativistic theory*, 3rd edition, Pergamon Press (1991).
- [38] J. D. Lykken, R. C. Myers and J. Wang, JHEP **0009**, 009 (2000) [arXiv:hep-th/0006191].
- [39] J. N. Fry, K. A. Olive and M. S. Turner, Phys. Rev. D **22**, 2953 (1980).
- [40] E. Kolb, M. Turner, *The Early Universe*, Addison-Wesley (1990).

- [41] D. N. Spergel *et al.* [WMAP Collaboration], *Astrophys. J. Suppl.* **170**, 377 (2007) [arXiv:astro-ph/0603449].
- [42] T. Han, J. D. Lykken and R. J. Zhang, *Phys. Rev. D* **59**, 105006 (1999) [arXiv:hep-ph/9811350].
- [43] H. Firouzjahi and S. H. Tye, *JHEP* **0601**, 136 (2006) [arXiv:hep-th/0512076].
- [44] O. DeWolfe, S. Kachru and H. L. Verlinde, *JHEP* **0405**, 017 (2004) [arXiv:hep-th/0403123].
- [45] P. Candelas and X. C. de la Ossa, *Nucl. Phys. B* **342**, 246 (1990).
- [46] B. v. Harling and A. Hebecker, arXiv:0801.4015 [hep-ph].